1   **Characteristics of PM$_{2.5}$ mass concentrations and chemical species in urban and background**

2   **areas of China: emerging results from the CARE-China network**

3   Zirui Liu[1*], Wenkang Gao[1], Yangchun Yu[1], Bo Hu[1], Jinyuan Xin[1], Yang Sun[1], Lili Wang[1], Gehui

4   Wang[3], Xinhui Bi[4], Guohua Zhang[4], Honghui Xu[5], Ziyuan Cong[6], Jun He[7], Jingsha Xu[7], Yuesi

5   Wang[1,2*]

6   [1]State Key Laboratory of Atmospheric Boundary Layer Physics and Atmospheric Chemistry, Institute of

7   Atmospheric Physics, Chinese Academy of Sciences, Beijing 100029, China

8   [2]Center for Excellence in Regional Atmospheric Environment, Institute of Urban Environment, Chinese Academy of

9   Sciences, Xiamen 361021, China

10   [3]State Key Laboratory of Loess and Quaternary Geology, Institute of Earth Environment, Chinese Academy of

11   Sciences, Xi'an 710075, China

12   [4]State Key Laboratory of Organic Geochemistry, Guangzhou Institute of Geochemistry, Chinese Academy of

13   Sciences, Guangzhou 510640, China

14   [5]Zhejiang Meteorology Science Institute, Hangzhou 310017, China

15   [6]Key Laboratory of Tibetan Environment Changes and Land Surface Processes, Institute of Tibetan Plateau

16   Research, Chinese Academy of Sciences, Beijing 100101, China

17   [7]International Doctoral Innovation Centre, The University of Nottingham Ningbo China, Ningbo, PR China

18   [*]Corresponding author: Z.R Liu (Liuzirui@mail.iap.ac.cn); Y.S Wang (wys@mail.iap.ac.cn)

19

20   **Abstract:** The "Campaign on atmospheric Aerosol REsearch" network of China (CARE-China) is

21   a long-term project for the study of the spatiotemporal distributions of physical aerosol

22   characteristics as well as the chemical components and optical properties of aerosols over China.

23   This study presents the first long-term datasets from this project, including three years of

24   observations of online PM$_{2.5}$ mass concentrations (2012-2014) and one year of observations of

25   PM$_{2.5}$ compositions (2012-2013) from the CARE-China network. The average PM$_{2.5}$

26   concentrations at 20 urban sites is 73.2 μg/m^3 (16.8-126.9 μg/m^3), which was three times higher

27   than the average value from the 12 background sites (11.2-46.5 μg/m^3). The PM$_{2.5}$ concentrations

28   are generally higher in east-central China than in the other parts of the country due to their relative

29   large particulate matter (PM) emissions and the unfavorable meteorological conditions for

30   pollution dispersion. A distinct seasonal variability of the PM$_{2.5}$ is observed, with highs in the

31   winter and lows during the summer at urban sites. Inconsistent seasonal trends were observed at

32   the background sites. Bimodal and unimodal diurnal variation patterns were identified at both

33   urban and background sites. The chemical compositions of PM$_{2.5}$ at six paired urban and

34   background sites located within the most polluted urban agglomerations and cleanest regions of

35   China were analyzed. The major PM$_{2.5}$ constituents across all the urban sites are organic matter

36   (OM, 26.0%), SO$_4^{2-}$ (17.7%), mineral dust (11.8%), NO$_3^-$ (9.8%), NH$_4^+$ (6.6%), elemental carbon

37   (EC) (6.0%), Cl$^-$ (1.2%) at 45% RH and residual matter (20.7%). Similar chemical compositions

38   of PM$_{2.5}$ were observed at background sites but were associated with higher fractions of OM

39   (33.2%) and lower fractions of NO$_3^-$ (8.6%) and EC (4.1%). Significant variations of the chemical

40   species were observed among the sites. At the urban sites, the OM ranged from 12.6 μg/m^3 (Lhasa)

41   to 23.3 μg/m^3 (Shenyang), the SO$_4^{2-}$ ranged from 0.8 μg/m^3 (Lhasa) to 19.7 μg/m^3 (Chongqing),

42   the NO$_3^-$ ranged from 0.5 μg/m^3 (Lhasa) to 11.9 μg/m^3 (Shanghai) and the EC ranged from 1.4

43 μg/m^3 (Lhasa) to 7.1 μg/m^3 (Guangzhou). The PM$_{2.5}$ chemical species at the background sites
44 exhibited larger spatial heterogeneities than those at urban sites, suggesting the different
45 contributions from regional anthropogenic or natural emissions and from the long-range transport
46 to background areas. Notable seasonal variations of PM$_{2.5}$ polluted days were observed, especially
47 for the megacities in east-central China, resulting in frequent heavy pollution episodes occurring
48 during the winter. The evolution of the PM$_{2.5}$ chemical compositions on polluted days was similar
49 for the urban and nearby background sites, suggesting the significant regional pollution
50 characteristics of the most polluted areas of China. However, the chemical species dominating the
51 evolutions of the heavily polluted events were different in these areas, indicating that unique
52 mitigation measures should be developed for different regions of China. This analysis reveals the
53 spatial and seasonal variabilities of the urban and background aerosol concentrations on a national
54 scale and provides insights into their sources, processes, and lifetimes.
55
56 **1. Introduction**
57   Atmospheric fine particulate matter (PM$_{2.5}$) is a complex heterogeneous mixture, whose
58 physical size distribution and chemical composition change in time and space and are dependent
59 on the emission sources, atmospheric chemistry, and meteorological conditions (Seinfeld and
60 Pandis, 2016). Atmospheric PM$_{2.5}$ has known important environmental impacts related to visibility
61 degradation and climate change. Because of their abilities to scatter and absorb solar radiation,
62 aerosols degrade visibility in both remote and urban locations and can have direct and indirect
63 effects on the climate (IPCC, 2013). Fine atmospheric particles are also a health concern and have
64 been linked to respiratory and cardiovascular diseases (Sun et al., 2010; Viana et al., 2008; Zhang
65 et al., 2014a). The magnitudes of the effects of PM$_{2.5}$ on all these systems depend on their sizes
66 and chemical compositions. Highly reflective aerosols, such as sulfates and nitrates, result in
67 direct cooling effects, while aerosols with low single-scattering albedos absorb solar radiation and
68 include light-absorbing carbon, humic-like substances, and some components of mineral soils
69 (Hoffer et al., 2006). The health impacts of these particles may also differ with different aerosol
70 compositions (Zimmermann, 2015); the adverse health effects specifically associated with organic
71 aerosols have been reported by Mauderly and Chow (2008). Therefore, the uncertainties
72 surrounding the roles of aerosols in climate, visibility, and health studies can be significant
73 because chemical composition data may not be available for large spatial and temporal ranges.
74   Reducing the uncertainties associated with aerosol effects requires observations of aerosol
75 mass concentrations and chemical speciation from long-term spatially extensive ground-based
76 networks. Continental sampling using ground-based networks has been conducted in North
77 America (Hand et al., 2012) and Europe (Putaud et al., 2010) since the 1980s, such as via the U.S.
78 EPA's Chemical Speciation Network (CSN), the Interagency Monitoring of Protected Visual
79 Environments (IMPROVE) network, the Clean Air Status and Trends Network (CASTNET) and
80 the National Atmospheric Deposition Program (NADP). Previous studies suggest the spatial and
81 temporal patterns of PM$_{2.5}$ mass concentrations and chemical species can vary significantly
82 depending on species and location. For example, Malm et al. (2004) reported the 2001 monthly
83 mean speciated aerosol concentrations from the IMPROVE monitors across the United States and
84 demonstrated that ammonium sulfate concentrations were highest in the eastern United States and

85 dominated the fine particle masses in the summer. Clearly decreasing gradients of the SO_4^{2-} and
86 NO_3^- contributions to PM_{10} were observed in Europe when moving from rural to urban to kerbside
87 sites (Putaud et al., 2010). Although large disparities of $PM_{2.5}$ pollution levels exist between those
88 megacities in developing and developed countries, the $PM_{2.5}$ annual mass concentrations in the
89 former are approximately 10 times greater than those of the latter (Cheng et al., 2016); however,
90 ground-based networks that consistently measures $PM_{2.5}$ mass concentrations and chemical
91 compositions remain rare in the densely populated regions of developing countries.

92   China is the world's most populous country and has one of the fastest-growing economies.
93 Fast urbanization and industrialization can cause considerable increases in energy consumption.
94 China's energy consumption increased 120% from 2000 to 2010. Coal accounted for most of the
95 primary energy consumption (up to 70%) (Department of Energy Statistics, National Bureau of
96 Statistics of China, 2001; 2011). Meanwhile, the emissions of high concentrations of numerous air
97 pollutants cause severe air pollution and haze episodes. For example, a heavy air pollution episode
98 occurred in northeastern China in January of 2013, wherein the maximum hourly averaged $PM_{2.5}$
99 exceeded 600 μgm^{-3} in Beijing (Wang et al., 2014). This event led to considerable public concern.
100 However, ground-based networks that consistently measure $PM_{2.5}$ mass concentrations and
101 chemical compositions in China are limited. Although there were some investigations of the
102 various aerosol chemical compositions in China (He et al., 2001; Huang et al., 2013; Li et al.,
103 2012; Liu et al., 2015; Pan et al., 2013; Tao et al., 2014; Wang et al., 2013; Yang et al., 2011; Zhao
104 et al., 2013a; Zhou et al., 2012), earlier studies were limited in their temporal and spatial scopes,
105 with very few having data exceeding one year while covering various urban and remote regions of
106 the country (Zhang et al., 2012; Wang et al., 2015). Indeed, before 2013, the Chinese national
107 monitoring network did not report measurements of $PM_{2.5}$ or its chemical composition, and thus,
108 ground-based networks for atmospheric fine particulate matter measurements at regional and
109 continental scales are needed as these networks are essential for the development and
110 implementation of effective air pollution control strategies and are also useful for the evaluation of
111 regional and global models and satellite retrievals.

112   To meet these sampling needs, the "Campaign on atmospheric Aerosol REsearch" network
113 of China (CARE-China) was established in late 2011 for the study of the spatiotemporal
114 distributions of the physical and chemical characteristics and optical properties of aerosols (Xin et
115 al., 2015). This study presents the first long-term dataset to include three years of observations of
116 online $PM_{2.5}$ mass concentrations (2012-2014) and one year of observations of $PM_{2.5}$ compositions
117 (2012-2013) from the CARE-China network. The purpose of this work is to (1) assess the $PM_{2.5}$
118 mass concentration levels, including the seasonal and diurnal variation characteristics at the urban,
119 rural and regional background sites; to (2) obtain the seasonal variations of the $PM_{2.5}$ chemical
120 compositions at paired urban/background sites in the most polluted regions and clean areas; and to
121 (3) identify the occurrences and chemical signatures of haze events via an analysis of the temporal
122 evolutions and chemical compositions of $PM_{2.5}$ on polluted days. These observations and analyses
123 provide general pictures of atmospheric fine particulate matter in China and can also be used to
124 validate model results and implement effective air pollution control strategies.

125 **2 Materials and methods**

126 **2.1 An introduction to the $PM_{2.5}$ monitoring sites**

127   The $PM_{2.5}$ data from 36 ground observation sites used in this study were obtained from the
128   CARE-China network (Campaign on the atmospheric Aerosol REsearch network of China), which
129   was supported by the Chinese Academy of Sciences (CAS) Strategic Priority Research Program
130   grants (Category A). Xin et al. (2015) provided an overview of the CARE-China network, the
131   cost-effective sampling methods employed and the post-sampling instrumental methods of
132   analysis. Four more ground observation sites (Shijiazhuang, Tianjin, Ji'nan and Lin'an) from the
133   "Forming Mechanism and Control Strategies of Haze in China" group (Wang et al., 2014) were
134   also included in this study to better depict the spatial distributions and temporal variations of the
135      $PM_{2.5}$ in eastern China. A comprehensive 3-year observational network campaign from 2012 to
136   2014 was carried out at these 40 ground observation sites. Figure 1 and Table 1, respectively, show
137   the geographic distribution and details of the network stations, which include 20 urban sites, 12
138   background sites and 8 rural/suburban sites. The urban sites, such as those at Beijing, Shanghai
139   and Guangzhou, are locations surrounded by typical residential areas and commercial districts.
140   The background sites are located in natural reserve areas or scenic spots, which are far away from
141   anthropogenic emissions and are less influenced by human activities. Rural/suburban sites are
142   situated in rural and suburban areas, which may be affected by agricultural activities, vehicle
143   emissions and some light industrial activities. These sites are located in different parts of China
144   and can provide an integrated insight into the characteristic of $PM_{2.5}$ over China.

145   **2.2 Online instruments and data sets**

146   A tapered element oscillating microbalance (TEOM) was used for the $PM_{2.5}$ measurements at
147   thirty-four sites within the network (Table S1). This system was designated by the US
148   Environmental Protection Agency (USEPA) as having a monitoring compliance equivalent to the
149   National Ambient Air Quality standard for particulate matter (Patashnick and Rupprecht 1991).
150   The measurement ranges of the TEOMs were 0-5 g/m^3, with a 0.1 $\mu g/m^3$ resolution and precisions
151   of ±1.5 (1-h average) and ±0.5 $\mu g/m^3$. The models used in the network are TEOM 1400 a and
152   TEOM 1405, and the entire system was heated to 50 ℃; thus, a loss of semivolatile compounds
153   cannot be avoided. Our previous study showed that up to 25% lower mass concentrations were
154   found for select daily means than those observed with gravimetric filter measurements, depending
155   on the ammonium-nitrate levels and ambient temperatures (Liu et al., 2015). The errors of the
156   TEOM measurements are systematic in that they are always negative. Thus, these errors may not
157   be important for the study of the spatial distributions and temporal variations of $PM_{2.5}$. The other
158   six sites of the network were equipped with beta gauge instruments (EBAM, Met One Instruments
159   Inc., Oregon) (Table S1). The measurement range of EBAM is 0-1000 $\mu g/m^3$, with a precision of
160   0.1 $\mu g/m^3$ and a resolution of 0.1 $\mu g/m^3$. The filters were changed every week, and the inlet was
161   cleaned every month. The flow rates were also monitored and concurrently calibrated.

162   **2.3 Filter sampling and chemical analysis**

163   In this study, filter sampling was conducted at the five urban sites of Beijing, Guangzhou,
164   Lhasa, Shenyang and Chongqing as well as at the six background sites of Xinglong, Lin'an,
165   Dinghu Mountain, Namsto, Changbai Mountain and Gongga Mountain. The Automatic Cartridge
166   Collection Unit (ACCU) system of Rupprecht & Patashnick Co. with 47 mm diameter quartz fiber
167   filters (Pall Life Sciences, Ann Arbor, MI, USA) was deployed in Beijing to collect the $PM_{2.5}$
168   samplers (Liu et al., 2016a). Similar to the ACCU system, a standard 47 mm filter holder with

169 quartz fiber filters (Pall Life Sciences, Ann Arbor, MI, USA) was placed in the bypass line of
170 TEOM 1400a and TEOM 1405 using quick-connect fittings and was used to collect the $PM_{2.5}$
171 samplers of the other nine sites, excepting Guangzhou and Lin'an. Each set of the $PM_{2.5}$ samples
172 was continuously collected over 48 h on the same days of each week, generally starting at
173 8:00 a.m. The flow rates were typically 15.6 L/min. For the Guangzhou site, the fine particles
174 were collected on Whatman quartz fiber filters using an Andersen model SA235 sampler
175 (Andersen Instruments Inc.) with an air flow rate of 1.13 m^3/min. The sampling lasted 24 or 48 h,
176 generally starting at 8:00 a.m. For the Lin'an site, a medium volume $PM_{2.5}$ sampler (Model:
177 TH-150CIII, Tianhong Instrument CO., Ltd. Wuhan, China) was used to collect 24 h of $PM_{2.5}$
178 aerosols on 90 mm quartz fiber filters (QMA, Whatman, UK) once every 6 days (Xu et al., 2017).
179 The sampling periods of these 11 urban and background sites are shown in Table S1.

180   All the filters were heat treated at 500 ℃ for at least 4 h for cleaning prior to filter sampling.
181 The $PM_{2.5}$ mass concentrations were obtained via the gravimetry method with an electronic
182 balance with a detection limit of 0.01 mg (Sartorius, Germany) after stabilizing at a constant
183 temperature (20±1 ℃) and humidity (45% ±5%). Three types of chemical species were measured
184 using the methods described in Xin et al. (2015). Briefly, the OC and elemental carbon (EC)
185 values were determined using a thermal/optical reflectance protocol using a DRI model 2001
186 carbon analyzer (Atmoslytic, Inc., Calabasas, CA, USA). Eight main ions, including K^+, Ca^{2+}, Na^+,
187 Mg^{2+}, NH_4^+, SO_4^{2-}, NO_3^- and Cl^-, were measured via ion chromatography (using a Dionex DX 120
188 connected to a DX AS50 autosampler for anions and a DX ICS90 connected to a DX AS40
189 autosampler for cations), and 18 elements, including Mg, Al, K, Ca, V, Cr, Mn, Fe, Co, Ni, Cu, Zn,
190 As, Se, Ag, Cd, Tl and Pb, were determined by Agilent 7500a inductively coupled plasma mass
191 spectrometry (ICP-MS, Agilent Technologies, Tokyo, Japan).

192

193 **3. Results and discussions**
194 **3.1 Characteristics of $PM_{2.5}$ mass concentrations at urban and background sites**
195 **3.1.1 Average $PM_{2.5}$ levels**
196   The location, station information and average $PM_{2.5}$ concentrations from the 40 monitoring
197 stations are shown in Fig. 1 and Table 1. The highest $PM_{2.5}$ concentrations were observed at the
198 urban stations of Xi'an (125.8 μg/m^3), Taiyuan (111.5 μg/m^3), Ji'nan (107.5 μg/m^3) and
199 Shijiazhuang (105.1 μg/m^3), which are located in the most polluted areas of the Guanzhong Plain
200 (GZP) and the North China Plain (NCP). Several studies have revealed that the enhanced $PM_{2.5}$
201 pollutions of the GZP and NCP are not only due to the primary emissions from local sources such
202 as the local industrial, domestic and agricultural sources but are also due to secondary productions
203 (Huang et al., 2014; Guo et al., 2014; Wang et al., 2014). Furthermore, the climates of the GZP
204 and NCP are characterized by stagnant weather with weak winds and relatively low boundary
205 layer heights, leading to favorable atmospheric conditions for the accumulation, formation and
206 processing of aerosols (Chan and Yao, 2008). Note that the averaged $PM_{2.5}$ concentrations in
207 Beijing and Tianjin were approximately 70 μg/m^3, which is much lower than those of the other
208 cities, including Ji'nan and Shijiazhuang in the NCP, possibly because Beijing and Tianjin are
209 located in the northern part of the NCP, far from the intense industrial emission area that is mainly
210 located in the southern part of the NCP. Interestingly, the average $PM_{2.5}$ concentrations at Yucheng

211 (102.8 μg/m^3) and Xianghe (83.7 μg/m^3) were even higher than most of those from the urban
212 stations. Although Yucheng is a rural site, it is located in an area with rapid urbanization near
213 Ji'nan and is therefore subjected to the associated large quantities of air pollutants. In addition,
214 Xianghe is located between Beijing and Tianjin and is influenced by the regionally transported
215 contributions from nearby megacities and the primary emissions from local sources. Yantai is a
216 coastal city with relatively low PM concentrations compared to those of with inland cities on the
217 NCP.

218   The PM$_{2.5}$ concentrations were also high in the Yangtze River Delta (YRD), which is another
219 developed and highly-populated city cluster area like the NCP (Fu et al., 2013). The average PM$_{2.5}$
220 values of the three urban stations of Shanghai, Wuxi and Hefei were 56.2, 65.2 and 80.4 μg/m^3,
221 respectively, which are comparable to those of the megacities of Beijing and Tianjin in the NCP.
222 Due to the presence of fewer coal-based industries and dispersive weather conditions, the PM$_{2.5}$
223 concentrations of the Pearl River Delta (PRD) are generally lower than those of the other two
224 largest city clusters in China, such as those from the NCP and YRD. The average PM$_{2.5}$ value at
225 Guangzhou was 44.1 μg/m^3, which was similar to the PM$_{2.5}$ values of the background stations
226 from the NCP and YRD. Shenyang, the capital of the province of Liaoning, is located in the
227 Northeast China Region (NECR), which is an established industrial area. High concentrations of
228 trace gases and aerosol scattering in the free troposphere have been observed via aircraft
229 observations and are due to regional transports and heavy local industrial emissions (Dickerson et
230 al., 2007). In the present study, the average PM$_{2.5}$ concentration of Shenyang was 77.6 μg/m^3.
231 Meanwhile, Hailun, which is a rural site in northeastern China, had an average PM$_{2.5}$
232 concentration of 41.6 μg/m^3, which was much lower than that of the rural site of Yucheng in the
233 NCP.

234   High aerosol optical depths and low visibilities have been observed in the Sichuan Basin
235 (Zhang et al., 2012), which is located in the Southwestern China Region (SWCR). The poor
236 dispersion conditions and heavy local industrial emissions make this another highly polluted area
237 in China. In the present study, the average PM$_{2.5}$ concentration in Chengdu was measured as 102.2
238 μg/m^3, which is much higher than the averages from the megacities of Beijing, Shanghai and
239 Guangzhou but is comparable to those of Ji'nan and Shijiazhuang. Chongqing, another megacity
240 located in the SWCR, however, showed much lower PM$_{2.5}$ values than Chengdu. Urumqi, the
241 capital of the Uighur Autonomous Region of Xinjiang, located in northwestern China, experiences
242 air pollution due to its increasing consumption of fossil fuel energy and steadily growing fleet of
243 motor vehicles (Mamtimin and Meixner, 2011). The average PM$_{2.5}$ concentration measured in
244 Urumqi is 104.1 μg/m^3, which is comparable to those of the urban sites in the GZP and NCP. The
245 similarity among the PM$_{2.5}$ values for Cele, Dunhuang and Fukang is due to their location, being
246 far from regions with intensive economic development but strongly affected by sandstorms and
247 dust storms due to their proximity to dust source areas. For example, the average PM$_{2.5}$
248 concentration in Cele during the spring (200.7 μg/m^3) was much greater than those of the other
249 three seasons. Lhasa, the capital of the Tibet Autonomous Region (TAR), is located in the center
250 of the Tibetan Plateau at a very high altitude of 3700 m. The PM$_{2.5}$ concentrations in Lhasa were
251 low, with average values of 30.6 μg/m^3, because of its relatively small population and few
252 industrial emissions.

253   Much lower $PM_{2.5}$ concentrations were observed at the background stations, the values of
254   which ranged from 11.2 to 46.5 μg/m^3. The lowest concentration of $PM_{2.5}$ was observed in Namsto,
255   a background station on the TAR with nearly no anthropogenic effects. The highest $PM_{2.5}$
256   concentration of the background stations was observed at Lin'an, a background station in the PRD.
257   The average $PM_{2.5}$ concentration at the urban and background sites in this study are shown as
258   box-plots in Fig. S1a. The average $PM_{2.5}$ concentration of the background stations (a total of 12
259   sites) is 28.5 μg/m^3, and the average concentration of the $PM_{2.5}$ values from urban stations (a total
260   of 20 sites) is 73.2μg/m^3. The latter value is approximately three times the former, suggesting the
261   large differences in fine particle pollution at urban and background sites across China. All values
262   were much greater than the results from Europe and North America. Gehrig and Buchmann (2003)
263   reported that average $PM_{2.5}$ concentrations from 1998 to 2001 at urban/suburban stations in
264   Switzerland were 20.1 μg/m^3. The average $PM_{2.5}$ concentrations were 16.3 μg/m^3 for the period
265   2008-2009 in the Netherlands (Janssen et al., 2013). Between October 2008 and April 2011, the 20
266   study areas of the European ESCAPE project showed annual average concentrations of $PM_{2.5}$
267   ranging from 8.5 to 29.3 μg/m^3, with low concentrations in northern Europe and high
268   concentrations in southern and eastern Europe (Eeftens et al., 2012). An average $PM_{2.5}$ value of
269   14.0 μg/m^3 was observed over the study period of 2000-2005 via measurements from 187 counties
270   in the United States, with higher values in the eastern United States and California and lower
271   values in the central regions and the northwest (Bell et al., 2007).
272   To further characterize these kinds of differences for different parts of China, six pairs of
273    $PM_{2.5}$ values measured from urban and background stations were selected to represent the NCP,
274   YRD, PRD, TAR, NECR and SWCR, respectively (Fig. S1). The first three areas (NCP, YRD and
275   PRD) and the last two areas (NECR and SWCR) were the most industrialized and populated
276   regions in China, while TAR is the cleanest area in China. The $PM_{2.5}$ concentrations of the
277   background stations in the NCP, YRD and PRD are 39.8 μg/m^3 (Xinglong), 46.5 μg/m^3 (Lin'an)
278   and 40.1 μg/m^3 (Dinghu Mountain) and are much higher than those of the background stations in
279   other parts of China, which are usually below 25 μg/m^3. In addition, the background $PM_{2.5}$
280   concentrations in the NCP, YRD and PRD were comparable to those from nearby urban sites,
281   especially for the PRD, as shown in Fig. S1. In contrast, the background $PM_{2.5}$ concentrations in
282   TAR, NECR and SWCR were much lower than those of the nearby cities. These results suggest
283   that the background sites in the NCP, YRD and PRD are more influenced by regional pollution,
284   which will be further discussed in section 3.2.
285   **3.1.2 Seasonal variations of $PM_{2.5}$ mass concentrations**
286   Generally, the $PM_{2.5}$ concentrations in urban areas show distinct seasonal variabilities, with
287   maxima during the winter and minima during the summer for most of China (Fig. 1), which is a
288   similar pattern to that of the results reported by Zhang and Cao (2015). In northern and
289   northeastern China, the wintertime peak values of $PM_{2.5}$ were mainly attributed to the combustion
290   of fossil fuels and biomass burning for domestic heating over extensive areas, which emit large
291   quantities of primary particulates as well as the precursors of secondary particles (He et al., 2001).
292   In addition, new particle formation and the secondary production of both inorganic aerosols and
293   OM could further enhance fine PM abundance (Huang et al., 2014; Guo et al., 2014). Furthermore,
294   the planetary boundary layer is relatively low in the winter, and more frequent occurrences of

295   stagnant weather and intensive temperature inversions cause very bad diffusion conditions, which
296   can result in the accumulation of atmospheric particulates and lead to high-concentration PM
297   episodes (Quan et al., 2014; Zhao et al., 2013b). In southern and eastern China, although the effect
298   of domestic heating is not as important as that in northern China, the weakened diffusion and
299   transport of pollutants from the north due to the activity of the East Asian Winter Monsoon
300   reinforces the pollution from large local emissions in the winter more than in any other season (Li
301   et al., 2011; Mao et al., 2017). For northwestern and West Central China, the most polluted season
302   is the spring instead of the winter due to the increased contribution from dust particles in this
303   desert-like region (Zou and Zhai, 2004), suggesting that the current $PM_{2.5}$ control strategies (i.e.,
304   reducing fossil/non-fossil combustion derived VOCs and PM emissions) will only partly reduce
305   the $PM_{2.5}$ pollution in western of China. $PM_{2.5}$ is greatly decreased during the summer in urban
306   areas, which is associated with the reduced anthropogenic emissions from fossil fuel combustion
307   and biomass burning domestic heating. Further, the more intense solar radiation causes a higher
308   atmospheric mixing layer, which leads to strong vertical and horizontal aerosol dilution effects
309   (Xia et al., 2006). In addition, increased precipitation in most of China due to the summer
310   monsoon can increase the wet scavenging of atmospheric particles. As a result, $PM_{2.5}$ minima are
311   observed in the summer at urban sites.
312   The seasonal variations of $PM_{2.5}$ at the background sites varied in different parts of China
313   (Fig. 3). Dinghu Mountain and Lin'an showed maximum values in the winter, while Zangdongnan,
314   Qinghai Lake, Xishuangbanna and Mount Everest showed maximum values in the spring. In
315   addition, a summer maximum of $PM_{2.5}$ was observed for Xinglong, and an autumn maximum was
316   observed for Tongyu. Changbai Mountain, Gongga Mountain and Namsto showed weak seasonal
317   variabilities. These results suggest the different contributions from regional anthropogenic and
318   natural emissions and long-range transports to background stations. The monthly average $PM_{2.5}$
319   concentrations of the urban and background sites in the NCP, YRD, PRD, TAR, NECR and SWCR
320   are further analyzed and shown in Fig. 2. The monthly variations of the $PM_{2.5}$ concentrations at
321   the background sites in the YRD and PRD were consistent with those of the nearby urban sites,
322   both of which showed maximum values in December (YRD) and January (PRD). The reasons for
323   this similarity are primarily the seasonal fluctuations of emissions, which are already well known
324   due to the similar variations of other parameters, including sulfur dioxide and nitrogen oxide, as
325   shown in Fig. S2. In contrast, the monthly variations of $PM_{2.5}$ at Xinglong showed different trends
326   than those of the nearby urban stations. The maximum value of $PM_{2.5}$ at this site was observed in
327   July, while the maximum value in Beijing was observed in January. The reasons for this are not
328   primarily the seasonal fluctuations of emissions, but rather meteorological effects (frequent
329   inversions during the winter and strong vertical mixing during the summer). The Xinglong site is
330   situated at an altitude of 900 m a.s.l., and therefore, during the wintertime, the majority of cases
331   above the inversion layer are protected from the emissions of the urban agglomerations of the NCP.
332   Furthermore, in the NCP area, northerly winds prevail in the winter, while southerly winds prevail
333   in the summer. Thus, in the summer, more air masses from the southern urban agglomerations will
334   lead to high $PM_{2.5}$ concentrations in Xinglong. Weak monthly variabilities were observed for
335   Namsto, Changbai Mountain and Gongga Mountain, although remarkable monthly variabilities
336   were found at the nearby cities of Lhasa, Shenyang and Chongqing. The reasons for this difference

337 are mainly that these three sites are elevated remote stations that are far from human activities and
338 show predominant meteorological influences.

3.1.3 Diurnal variations of PM$_{2.5}$ mass concentrations

340 To derive importance information to identify the potential emission sources and the times
341 when the pollution levels exceed the proposed standards, hourly data were used to examine the
342 diurnal variabilities of PM$_{2.5}$ as well as those of the other major air pollutants. Fig. 3 illustrates the
343 diurnal variations of the hourly PM$_{2.5}$ concentrations in Beijing, Shanghai, Guangzhou, Lhasa,
344 Shenyang and Chongqing, in the largest megacities in the NCP, YRD, PRD, TPR, NECR and
345 SWCR and in the different climatic zones of China, respectively. Of the urban sites, Lhasa has the
346 lowest PM$_{2.5}$ concentrations, but the most significant pronounced diurnal variations of PM$_{2.5}$, with
347 obvious morning and evening peaks appearing at 10:00 and 22:00 (Beijing Time)due to the
348 contributions of enhanced anthropogenic activity during the rush hours. The minimum value
349 occurred at 16:00, which is mainly due to a higher atmospheric mixing layer, which is beneficial
350 for air pollution diffusion. This bimodal pattern was also observed in Shenyang and Chongqing,
351 which show morning peaks at 7:00 and 9:00 and evening peaks at 19:00 and 20:00, respectively.
352 However, the PM$_{2.5}$ values in Beijing, Shanghai and Guangzhou showed much weaker urban
353 diurnal variation patterns, and slightly higher PM$_{2.5}$ concentrations during the night than during
354 the day were observed, which can be explained by the enhanced emissions from heating and the
355 relatively low boundary layer. Note that the morning peaks in Beijing, Shanghai and Guangzhou
356 were not as obvious as those of other cities, although both the SO$_2$ and NO$_2$ values increased due
357 to increased anthropogenic emissions (Fig. S3). Alternatively, this decreasing trend may be the
358 result of an increasing boundary layer depth. At these three urban sites, the PM$_{2.5}$ levels started to
359 increase in the late afternoon, which could be explained by the increasing motor vehicle emissions
360 as NO$_2$ is also dramatically increased during the same period.

361 At the background area of the TPR, significant pronounced diurnal variations of PM$_{2.5}$ were
362 observed in Namsto, with a morning peak at 9:00 and an evening peak at 21:00 (Fig. 3d), which
363 are similar to those of the urban site of Lhasa. As there are hardly any anthropogenic activities
364 near Namsto, this kind of diurnal pattern of PM$_{2.5}$ may be influenced by the evolution of the
365 planetary boundary layer. Both Lin'an and Gongga Mountain showed the same bimodal pattern of
366 PM$_{2.5}$ as that in Namsto, which could also be influenced by the planetary boundary layer. For the
367 background site of the NCP, however, Xinglong showed smooth PM$_{2.5}$ variations. As mentioned
368 before, the Xinglong station is located on the mountain and has an altitude of 960 m a.s.l. The
369 mixed boundary layer of the urban area increases in height in the morning and reaches a height of
370 approximately 1000 meters in the early afternoon. Then, the air pollutants from the urban area
371 start to affect the station as the vertical diffusion of the airflow and the PM$_{2.5}$ concentration reach
372 their maxima at 18:00. Next, the concentration starts to decrease when the mixed boundary layer
373 collapses in the late afternoon, eventually forming the nocturnal boundary layer (Boyouk et al.,
374 2010). Thus, PM$_{2.5}$ concentration decreased slowly during the night and morning, reaching a
375 minimum at 10:00. At Dinghu Mountain and Changbai Mountain, the daytime PM$_{2.5}$ greater than
376 that of the nighttime, with a maximum value occurring at approximately 11:00-12:00. This kind of
377 diurnal pattern of PM$_{2.5}$ is mainly determined by the effects of the mountain-valley breeze. Both
378 the Dinghu Mountain and Changbai Mountain stations are located near the mountain. Thus, during

379　daytime, the valley breeze from urban areas carries air pollutants that will accumulate in front of
380　the mountain and cause an increase of the PM concentration. Meanwhile, at night, the fresh air
381　carried by the mountain breeze will lead to the dilution of the PM, so low concentrations are
382　sustained during the night. Further support for this pattern comes from the much higher maximum
383　values of $PM_{2.5}$ in the winter than those in the summer, as enhanced air pollutant emissions in
384　urban areas are expected in the winter due to heating.

385　**3.2 Chemical compositions of $PM_{2.5}$ in urban and background sites**

386　**3.2.1 Overview of $PM_{2.5}$ mass speciation**

387　　　　Figure 4 shows the annual average and seasonal average chemical compositions of $PM_{2.5}$ at
388　six urban and six background sites, which represent the largest megacities and regional
389　background areas of the NCP, YRD, PRD, TPR, NECR and SWCR. The chemical species of
390　$PM_{2.5}$ in Shanghai were obtained from Zhao et al. (2015). The atmospheric concentrations of the
391　main $PM_{2.5}$ constituents are also shown in Table 2. The EC, nitrate (NO_3^-), sulfate (SO_4^{2-}),
392　ammonium (NH_4^+) and chlorine (Cl^-) concentrations were derived directly from measurements.
393　Organic matter (OM) was calculated assuming an average molecular weight per carbon weight,
394　showing an OC of 1.6 at the urban sites and of 2.1 at the background sites, based on the work of
395　Turpin and Lim (2001); however, these values are also spatially and temporally variable, and
396　typical values could range from 1.3 to 2.16 (Xing, et al., 2013). The calculation of mineral dust
397　was performed on the basis of crustal element oxides (Al_2O_3, SiO_2, CaO, Fe_2O_3, MnO_2 and K_2O).
398　In addition, the Si content, which was not measured in this study, was calculated based on its ratio
399　to Al in crustal materials; namely, $[Si]=3.41\times[Al]$. Finally, the unaccounted-for mass refers to the
400　difference between the $PM_{2.5}$ gravimetric mass and the sum of the PM constituents mentioned
401　above.

402　　　　The PM constituents' relative contributions to the PM mass are independent of their
403　dilutions and reflect differences in the sources and processes controlling the aerosol compositions
404　(Putaud et al., 2010). When all the main aerosol components except water are quantified, they
405　account for 73.6-84.8% of the $PM_{2.5}$ mass (average 79.2%) at urban sites and for 76.2-91.1% of
406　the $PM_{2.5}$ mass (average 83.4%) at background sites. The remaining unaccounted-for mass fraction
407　may be the result of analytical errors, a systematic underestimation of the PM constituents whose
408　concentrations are calculated from the measured data (e.g., OM, and mineral dust), and
409　aerosol-bound water (especially when mass concentrations are determined at RH >30%). For the
410　urban sites, the mean composition given in descending concentrations is 26.0% OM, 17.7% SO_4^{2-},
411　11.8% mineral dust, 9.8% NO_3^-, 6.6% NH_4^+, 6.0% EC and 1.2% Cl^-. For the background sites, the
412　mean composition given in descending concentrations is 33.2% OM, 17.8% SO_4^{2-}, 10.1% mineral
413　dust, 8.7% NH_4^+, 8.6% NO_3^-, 4.1% EC and 0.9% Cl^-. Generally, the chemical compositions of the
414　$PM_{2.5}$ at background sites are similar to those of the urban sites, although they show a much higher
415　fraction of OM and lower fractions of NO_3^- and EC. Significant seasonal variations of the
416　chemical compositions were observed at urban sites (Fig. 4c), with much higher fractions of OM
417　(33.7%) and NO_3^- (11.1%) in the winter and much lower fractions of OM (20.7%) and NO_3^- (6.9%)
418　in the summer. In contrast, the fraction of SO_4^{2-} was consistent among the different seasons,
419　although its absolute concentration in the winter (14.9 μg/m^3) was higher than that in the summer
420　(11.7 μg/m^3). Compared with those at urban sites, different seasonal variation of OM were

421 observed at the background sites, which showed summer maxima and winter/spring minima (Fig.
422 4d). While the wintertime peaks of OM at the urban sites were probably due to additional local
423 emissions sources related to processes like heating, the summer peaks at the background sites were
424 attributed to the enhanced biogenic emissions. Note that the seasonal variations of NO_3^- were
425 similar to those at urban sites; this seasonal phenomenon is due to the favorable conditions of cold
426 temperature and high relative humidity conditions leading to the formation of particulate nitrate.
427 The seasonal behaviors of SO_4^{2-} at the background sites were markedly different than those of the
428 urban sites and indicate very different sources and atmospheric processing of SO_4^{2-}, which will be
429 further discussed for specific regions of China.

430 There are significant variations of the absolute speciation concentrations at these urban and
431 background sites (Table 2). For the urban sites, the OM concentrations span a 2-fold concentration
432 range from 12.6 $\mu g/m^3$ (Lhasa) to 23.3 $\mu g/m^3$ (Shenyang), while these values range from 3.4
433 $\mu g/m^3$ (Namtso) to 21.7 $\mu g/m^3$ (Lin'an) at the background sites. The SO_4^{2-} and NO_3^- concentrations
434 exhibit larger spatial heterogeneities than those of the OM for both urban and background sites.
435 The absolute values of SO_4^{2-} have an approximately 25-fold range in urban sites, from 0.8 $\mu g/m^3$
436 (Lhasa) to 19.7 $\mu g/m^3$ (Chongqing), while this value has a 30-fold range at the background sites,
437 from 0.4 $\mu g/m^3$ (Namsto) to 11.2 $\mu g/m^3$ (Lin'an). The corresponding mass fractions are 26.8% in
438 Chongqing and below 3% in Lhasa. Much higher fractions of SO_4^{2-} in the $PM_{2.5}$ were observed at
439 the urban sites located in southern China than those in northern China, although the average
440 concentration of $PM_{2.5}$ is greater in the north than in the south, suggesting that sulfur pollution
441 remains a problem for southern China (Liu, et al., 2016b). This problem may be attributed to
442 higher sulfur contents of the coal in southern China, with 0.51% in the north vs. 1.32% in the
443 south and up to >3.5% in Chongqing in southern China (Lu et al., 2010; Zhang et al., 2010). The
444 absolute values of NO_3^- have an approximately 20-fold range in urban sites and a greater than
445 100-fold range in background sites. This heterogeneity reflects the large spatial and temporal
446 variations of the NOx sources. For the urban sites, the absolute EC values have a 5-fold
447 concentration range, from 1.4 $\mu g/m^3$ (Lhasa) to greater than 7.0 $\mu g/m^3$ (Guangzhou), while this
448 species has a 15-fold concentration range at the background sites and is mainly from
449 anthropogenic sources. In comparison, the absolute concentrations of mineral dust exhibit much
450 weaker spatial variations at the urban and background sites.

451 The characteristics of the $PM_{2.5}$ chemical compositions at individual site were discussed in
452 more detail. In this section, six pairs of urban and background sites from each region of China
453 were selected, and the differences in the chemical compositions of urban and background sites
454 were analyzed.

3.2.2 North China Plain

456 Beijing is the capital of China and has attracted considerable attention due to its air pollution
457 (Chen et al., 2013). Beijing is the largest megacity in the NCP, which is surrounded by the
458 Yanshan Mountains to the west, north and northeast and is connected to the Great North China
459 Plain to the south. The filter sampler is located in the courtyard of the Institute of Atmospheric
460 Physics (IAP) (116.37 °E, 39.97 °N), 8 km northwest of the center of downtown. The $PM_{2.5}$
461 concentration during the filter sampling period was 71.7 $\mu g/m^3$, which is close to the three-year
462 average $PM_{2.5}$ value reported by TEOM (Table 1). $PM_{2.5}$ in Beijing is mainly composed by OM

463 (26.6%), SO_4^{2-} (16.5%) and NO_3^- (13.0%) (Fig. 5a), which compare well with previous studies
464 (Yang et al., 2011; Oanh et al., 2006). However, the mineral dust fraction found in this study
465 (6.5%) was much lower than that found in Yang et al. (2011) (19%) but was comparable to that
466 found in Oanh et al. (2006) (5%), potentially due to difference in definitions. The annual
467 concentration of OM (19.1 $\mu g/m^3$) in Beijing was comparable to those in Shanghai, Guangzhou
468 and Chongqing, but was much lower than that in Shenyang. Higher fractions of OM were
469 observed in the winter (34.2%) and autumn (30.5%) than in the summer (21.6%) and spring
470 (20.9%). The annual concentration of SO_4^{2-} (11.9 $\mu g/m^3$) was much lower than those of earlier
471 years (15.8 $\mu g/m^3$, 2005-2006) (Yang et al., 2011), suggesting that the energy structure adjustment
472 implemented in Beijing (e.g., replacing coal fuel with natural gas) has been effective in decreasing
473 the particulate sulfate in Beijing. Further support for this comes from the SO_4^{2-} concentration in
474 the winter (16.5 $\mu g/m^3$) being comparable to that in the summer (13.4 $\mu g/m^3$). The significant
475 NO_3^- value (9.3 $\mu g/m^3$) reflects the significant urban NOx emissions in Beijing, which was
476 greatest during the winter, as expected from ammonium-nitrate thermodynamics. The greater
477 mineral component in the spring reflects the regional natural dust sources.
478 The filter sampling site in Xinglong (117.58 °E, 40.39 °N) was located at Xinglong
479 Observatory, National Astronomical Observatory, Chinese Academy of Sciences, which is 110 km
480 northeast of Beijing (Fig. 1). This site is surrounded by mountains and is minimally affected by
481 anthropogenic activities. The PM$_{2.5}$ concentration during the filter sampling period was 42.6 $\mu g/m^3$,
482 which is close to the three-year average PM$_{2.5}$ values reported by TEOM (Table 1). The annual
483 chemical composition of the PM$_{2.5}$ in Xinglong was similar to that in Beijing, although relatively
484 higher fractions of OM and sulfate were observed in Xinglong (Fig. 5a). Higher fractions of OM
485 were found in the winter (36.7%), and higher fractions of sulfate were found in the summer
486 (32.1%) than in any other season (OM: 23.0-30.4%; SO_4^{2-}: 15.7-20.1%). Interestingly, the summer
487 SO_4^{2-} concentration in Xinglong (14.4 $\mu g/m^3$) was even higher than that in Beijing, suggesting
488 spatially uniform distributions of SO_4^{2-} concentrations across the NCP. This result indicates that
489 regional transport can be an important source of SO_4^2 aerosols in Beijing, especially during the
490 summer.

491 **3.2.3 Yangtze River Delta**

492 Shanghai is the economic center of China, lying on the edge of the broad flat alluvial plain of
493 the YRD, with a few mountains to the southwest. The filter sampler was located at the top of a
494 four-floor building of the East China University of Science and Technology (121.52 °E, 31.15 °N)
495 (Zhao et al., 2015), approximately 10 km northwest of the center of downtown. The PM$_{2.5}$
496 concentration during the filter sampling period was 68.4 $\mu g/m^3$, which is greater than the
497 three-year average PM$_{2.5}$ value reported by EBAM, likely due to the different sampling period
498 (Table S1). The PM$_{2.5}$ in Shanghai mainly comprises OM (24.9%), SO_4^{2-} (19.9%) and NO_3^-
499 (17.4%), which is comparable to the results of previous studies (Ye et al., 2003; Wang et al., 2016).
500 This site had the highest NO_3^- (11.9 $\mu g/m^3$) and the second-highest SO_4^{2-} (13.6 $\mu g/m^3$) values of
501 the urban sites, while its OM (17.1 $\mu g/m^3$) was comparable to those of Guangzhou and Chongqing.
502 The SO_4^{2-} and NO_3^- values were highest during the autumn as expected based on the widespread
503 biomass burning in the autumn in the YRD (Niu et al., 2013). However, the OM values were
504 highest during the winter and mainly originated from secondary aerosol processes based on the

505　highest OC/EC ratios (6.0) and the poor relationship of the OC and EC in this season.

506　　　　Filter sampling was conducted at the Lin'an Regional Atmospheric Background Station

507　(119.73 °E, 30.30 °N), which is a background monitoring station for the World Meteorological

508　Organization (WMO) global atmospheric observation network. The Lin'an site was located at the

509　outskirts of Lin'an County within Hangzhou Municipality, which was 200 km southwest of

510　Shanghai (Fig. 1). This site is surrounded by agricultural fields and woods and is less affected by

511　urban, industrial and vehicular emissions (Xu et al., 2017). The $PM_{2.5}$ concentration during the

512　filter sampling period was 66.3 μg/m^3, which is higher than the three-year average $PM_{2.5}$ values

513　reported by TEOM, likely due to the different sampling period (Table S1). The annual chemical

514　composition of the $PM_{2.5}$ in Lin'an was different than that in Shanghai, with much higher fractions

515　of OM (32.7%) and NH_4^+ (11.0%). Furthermore, the absolute concentration of OM in Lin'an was

516　much higher than that in Shanghai, especially in the summer (21.7 vs. 9.9 μg/m^3), which may be

517　attributed to the enhanced biomass burning at both local and regional scales as well as the higher

518　concentration of summer EC in Lin'an than in Shanghai (2.2 vs. 1.4 μg/m^3). In addition, the SO_4^{2-}

519　and NO_3^- concentrations in Lin'an were comparable to those in Shanghai. These results suggest a

520　spatially homogeneous distribution of secondary aerosols over the PRD and the the transportation

521　of aged aerosol and gas pollutants from city clusters has significantly changed the aerosol

522　chemistry in the background area of this region.

523　**3.2.4 Pearl River Delta**

524　　　Guangzhou is the biggest megacity in south China located in the PRD and mainly consists of

525　floodplains within the transitional zone of the East Asian monsoon system (Yang et al., 2011). The

526　filter sampler was set up on the rooftop of a 15-m high building of the Guangzhou Institute of

527　Geochemistry, Chinese Academy of Sciences (113.35 °E, 23.12 °N). This site was surrounded by

528　heavily trafficked roads and dense residential areas, representing a typical urban location. The

529　$PM_{2.5}$ concentration during the filter sampling period was 75.3 μg/m^3, which is much higher than

530　the three-year average $PM_{2.5}$ value reported by EBAM (Table 1), likely due to the different

531　sampling period and location. The $PM_{2.5}$ in Guangzhou mainly comprises OM (22.2%), SO_4^{2-}

532　(17.3%) and mineral dust (9.7%), which have values comparable to previous studies conducted in

533　the years of 2013-2014 (Chen et al., 2016; Tao et al., 2017). This site has the lowest OC/EC ratio

534　(1.5) of all urban sites, which can be explained by the abundance of diesel engine truck in

535　Guangzhou City (Verma et al., 2010). Obvious seasonal variations of OM, SO_4^{2-} and NO_3^- were

536　observed, showing winter/autumn maxima and summer/spring minima. In addition, summer

537　minima were also observed for EC and NH_4^+. High mixing heights in the summer and clean air

538　masses affected by summer monsoons from the South China Sea should lead to the minima of

539　these species in summer, while the low wind speeds, weak solar radiation, relatively low

540　precipitation (Tao et al., 2014) and relatively high emissions (Zheng et al., 2009) result in the

541　much higher concentrations of OM and secondary inorganic aerosols (SO_4^{2-}, NO_3^- and NH_4^+) in

542　the winter and autumn.

543　　　　Filter sampling was conducted at Dinghu Mountain Station (112.50 °E, 23.15 °N), which is

544　located in the middle of Guangdong Province in southern China. This site was surrounded by hills

545　and valleys, being approximately 70 km west of Guangzhou (Fig. 1). The $PM_{2.5}$ concentration

546　during the filter sampling period was 40.1 μg/m^3, close to the three-year average $PM_{2.5}$ values

547   reported by TEOM. Distinct seasonal variations of OM, SO_4^{2-}, NO_3^- and NH_4^+ were observed,

548   with the highest concentration of OM and NO_3^- occurring in the winter, while the highest

549   concentrations of SO_4^{2-} and NH_4^+ occurred in the autumn. In contrast, EC and mineral dust showed

550   weak seasonal variations. Dinghu Mountain has the second-highest EC and SO_4^{2-} values of the

551   background sites, being 2.0 μg/m^3 and 10.1 μg/m^3. In addition, the lowest OC/EC ratio was

552   observed at Dinghu Mountain (2.8); the other background sites had values ranging from 3.5-8.3.

553   These results indicate that this background site is intensely influenced by vehicular traffic, fossil

554   fuel combustion and industrial emissions due to the advanced urban agglomeration in the PRD

555   region. These results are consistent with the finds from previous studies (Liu et al., 2011; Wu et al.,

556   2016). Compared with those from Guangzhou, higher fractions of SO_4^{2-} and NO_3^- were observed

557   at Dinghu Mountain, while the fractions of OM and mineral dust were similar at these two sites,

558   possibly indicating that there was a significantly larger fraction of transported secondary aerosols

559   or aged aerosols at the background site of the PRD.

560 **3.2.5 Tibetan Autonomous Region**

561   Located in the inland TAR, Lhasa is one of the highest cities in the world (at an altitude of

562   3700 m). The city of Lhasa is located in a narrow west-east oriented valley in the southern part of

563   the TAR. The filter sampler was located on the roof of a 20-m high building on the campus of the

564   Institute of Tibetan Plateau Research (Lhasa branch) (91.63 °E, 29.63 °N). This site is close to

565   Jinzhu road, one of the busiest roads in the city (Cong et al., 2011). The $PM_{2.5}$ concentration

566   during the filter sampling period was 36.4 μg/m^3, which is close to the three-year average $PM_{2.5}$

567   values reported by TEOM. The $PM_{2.5}$ in Lhasa mainly comprises OM (34.5%) and mineral dust

568   (31.9%), and the secondary inorganic aerosols (SO_4^{2-}, NO_3^- and NH_4^+) contributed little to the

569     $PM_{2.5}$ (<5%). These results are comparable to those of a previous study conducted in the year of

570   2013-2014 (Wan et al., 2016). In addition, this site reports the lowest OM (12.6 μg/m^3), secondary

571   inorganic aerosols (1.7 μg/m^3) and EC (1.4 μg/m^3) values of the urban sites in this study. Higher

572   fractions of OM were observed in the winter (48.4%) and spring (43.1%), exceeding those in the

573   summer (24.6%) and autumn (31.2%). Weak seasonal variations were found for the SO_4^{2-}

574   (1.5-3.0%) and NO_3^- (1.1-1.7%) values, suggesting the negligible contributions from fossil fuel

575   combustion in Lhasa.

576   Filter sampling was conducted at the Namtso Monitoring and Research Station for

577   Multisphere Interactions (90.98 °E, 30.77 °N), a remote site located on the northern slope of the

578   Nyainqen-tanglha Mountains, approximately 125 km northwest of Lhasa (Fig. 1). The $PM_{2.5}$

579   concentration during the filter sampling period was 9.5 μg/m^3, which is close to the three-year

580   average $PM_{2.5}$ value reported by TEOM. The $PM_{2.5}$ in Namtso mainly comprises mineral dust

581   (40.8%) and OM (36.3%), while SO_4^{2-} and NO_3^- contributed less than 5% to the $PM_{2.5}$. This

582   chemical composition is distinctly different from those of the other background sites in this study,

583   but is comparable to the background site at Qinghai Lake in the TAR (Zhang et al., 2014b).

584   Namtso has the lowest OM, EC, SO_4^{2-}, NO_3^- and NH_4^+ values of all the background sites in this

585   study. Spring maxima and winter minima were observed for the OM and EC, while the SO_4^{2-},

586   NO_3^- and NH_4^+ values showed weak seasonal variations. The highest OC/EC ratio was observed

587   (8.3) at this site, suggesting that the organic aerosols at Namtso mainly originated from secondary

588   aerosol processes or aged organic aerosols from regional transports.

589 **3.2.6 Northeast China Region**

590   Shenyang is the capital city of Liaoning province and the largest city in northeastern China.
591 The main urban area is located on a delta to the north of the Hun River. The filter sampler was
592 located at the Shenyang Ecological Experimental Station of the Chinese Academy of Science
593 (123.40 °E, 41.50 °N) and was surrounded by residential areas with no obvious industrial pollution
594 sources around the monitoring station, representing the urban area of Shenyang. The $PM_{2.5}$
595 concentration during the filter sampling period was 81.8 μg/m^3, which is close to the three-year
596 average $PM_{2.5}$ value reported by TEOM (Table 1). The $PM_{2.5}$ in Shenyang mainly comprises OM
597 (28.5%), SO_4^{2-} (16.1%) and mineral dust (11.3%). This site reports the highest OM (23.3 μg/m^3)
598 and mineral dust (9.2 μg/m^3) values as well as the second-highest EC (5.2 μg/m^3) value of the
599 urban sites. The NO_3^- concentration at this site, however, was the second-lowest of the urban sites
600 (Table 2). Much higher fractions of OM were observed in the winter (40.5%) than in the other
601 seasons (15.6-26.5%) (Fig. 5), possibly due to the enhanced coal burning for winter heating.
602 Further support for this pattern comes from the high abundance of chlorine during the cold seasons,
603 which is mainly associated with coal combustion. The contribution from sea-salt particles is not
604 important since the sampling sites are at least 200 km from the sea. Note that the fraction of SO_4^{2-}
605 in the $PM_{2.5}$ during the winter was lower than that in the summer, although the absolute
606 concentration was much higher in the winter (23.6 μg/m^3) than in the summer (11.3 μg/m^3). This
607 result may be attributed to the reduced transformation of sulfur dioxide at low temperatures.

608   Filter sampling was conducted at the Changbai Mountain forest ecosystem station
609 (128.01 °E, 42.40 °N), which was mostly surrounded by hills and forest and is located
610 approximately 390 km northeast of Shenyang (Fig. 1). This site is situated 10 km from the nearest
611 town, Erdaobaihe, which has approximately 45000 residents. The sources of PM were expected to
612 be non-local. Hence, this site is considered a background site in the NECR. The $PM_{2.5}$
613 concentration during the filter sampling period was 23.3 μg/m^3, which is close to the three-year
614 average $PM_{2.5}$ value reported by TEOM (Table 1). The main contributions to the $PM_{2.5}$ at
615 Changbai Mountain were OM (38.1%), mineral dust (16.0%) and SO_4^{2-} (14.3%), similar to those
616 in Shenyang. Note that the summer OM concentrations were quite similar at these two sites (8.0 vs.
617 9.0 μg/m^3), but the OC/EC ratios were different (4.8 vs. 1.6), which may reflect the different
618 origins of the OM at the urban (primary emissions) and background sites (secondary processes) of
619 the NECR. The OM concentrations in the other seasons were much lower at Changbai Mountain
620 than those from Shenyang city, especially during the winter (10.8 vs. 59.4 μg/m^3). In fact, weak
621 seasonal variations of chemical species (OM, EC, SO_4^{2-}, NO_3^- and NH_4^+) were observed at
622 Changbai Mountain. This site reports the second-lowest values of OM, EC, SO_4^{2-} and Cl$^-$ of the
623 background sites. These results suggest that aerosols at Changbai Mountain were influenced by
624 the regional transports alone.

625 **3.2.7 Southwestern China Region**

626   Chongqing is the fourth municipality near Central China, lying on the Yangtze River in
627 mountainous southwestern China, near the eastern border of the Sichuan Basin and the western
628 border of Central China. For topographic reasons, Chongqing has some of the lowest wind speeds
629 in China (annual averages of 0.9-1.6 m s^{-1} from 1979 to 2007; Chongqing Municipal Bureau of
630 Statistics, 2008), which favors the accumulation of pollutants. The filter sampler was located on

the rooftop of a 15-m high building on the campus of the Southwest University (106.54 °E, 29.59 °N). This site is located in an urban district of Chongqing with no obvious industrial pollution sources around the monitoring site, representing the urban area of Chongqing. The $PM_{2.5}$ concentration during the filter sampling period was 73.5 μg/m^3, of which 26.8% is SO_4^{2-}, 23.5% OM, 10.0% mineral dust, 8.9% NO_3^-, 8.2% EC and 6.5% NH_4^+. The OM fraction is smaller than those measured by Yang et al. (2011) (32.7%) and Chen et al., 2017 (30.8%), while the SO_4^{2-} fraction is greater than the values reported in these two studies (19.8-23.0%). This site shows the highest SO_4^{2-} (19.7 μg/m^3), the highest NH_4^+ (6.1 μg/m^3) and the third-highest EC (4.8 μg/m^3) values of the urban sites. A weak seasonal variation in the chemical composition of $PM_{2.5}$ was observed, although a much higher concentration of this species was found in the winter than in the other seasons.

Filter sampling was performed at the Gongga Mountain Forest Ecosystem Research Station (101.98 °E, 29.51 °N) in the Hailuogou Scenic Area, a remote site located in southeastern Ganzi in the Tibetan Autonomous Prefecture in Sichuan province. This site is mostly surrounded by glaciers and forests and is located approximately 450 km northwest of Chongqing (Fig. 1). The $PM_{2.5}$ concentration during the filter sampling period was 32.2 μg/m^3, close to the three-year average $PM_{2.5}$ value reported by TEOM (Table 1). The dominant components of $PM_{2.5}$ were OM (40.7%), SO_4^{2-}(14.6%) and mineral dust (9.8%), similar to those at Changbai Mountain. This site has the second-highest OM (13.1 μg/m^3) value of the background sites, which may mainly be due to secondary processes, considering the high OC/EC ratio (5.6). In addition, distinct seasonal variations of OM were observed, which shows summer maxima (19.9 μg/m^3) and autumn minima (9.1 μg/m^3). Previous studies showed higher mixing ratios of the VOCs during the spring and summer and lower mixing ratios during the autumn at Gongga Mountain (Zhang et al., 2014c), which may result in high concentrations of OM in the summer because the OC/EC ratio reaches its highest value in the summer (10.3). Second-lowest EC and NO_3^- values of the background sites were observed here, suggesting the insignificant influence of human activities in this region.

3.3 Temporal evolution and chemical composition $PM_{2.5}$ in polluted days

Using the "Ambient Air Quality Standard" (GB3095-2012) of China (CAAQS), the occurrences of polluted days exceeding the daily threshold values during 2012-2014 were counted for each site (Fig. 6). Based on the number of polluted days exceeding the CAAQS daily guideline of 35 μg/m^3, substandard days of $PM_{2.5}$ account for more than 60% of the total period at the majority of urban sites, excepting Lhasa, Taipei and Sanya. Note that the ten most polluted cities (Ji'nan, Chengdu, Taiyuan, Hefei, Shenyang, Xi'an, Changsha, Shijiazhuang, Wuxi and Chongqing) experienced less than 20% clean days (daily $PM_{2.5}$<35 μg/m^3) during the three-year observation period. Interestingly, the occurrences of heavily polluted days (daily $PM_{2.5}$>150 μg/m^3) were different among these ten most polluted cities. While more than 15% of the total period comprised heavily polluted days in Ji'nan, Taiyuan, Chengdu, Xi'an and Shijiazhuang, heavily polluted days accounted for less than 5% of the total days in the other five cities, which mainly experienced slightly polluted (35-75 μg/m^3) and moderately polluted (75-115 μg/m^3) days. Due to the regional pollutant transports, the rural and background sites near the most polluted cities also showed high occurrences of polluted days. Polluted days accounted for more than 50% of the total period at Xin'long, Lin'an and Dinghu Mountain. In addition, an even higher occurrence of polluted days

673 (>80%) was found for the rural areas of Yucheng and Xianghe. In contrast, the background sites in
674 the TAR, NECR and SWCR rarely experienced polluted days, and over 80% of the total period
675 comprised clean days at these sites.

676   The polluted days were not equally distributed throughout the year. The monthly distributions
677 for the polluted days at each site are shown in Fig. 7. In terms of the occurrences of heavily
678 polluted days, December, January and February were predominant months for the urban sites
679 located in the most polluted areas of the GZP and NCP, where both the unfavorable dispersion
680 conditions for pollutants and the additional emission enhancements from residential heating
681 contributed to the heavy pollution in the winter. The heavy pollution occurring in April and
682 November in Cele was primarily caused by sandstorms and dust storms. Heavily polluted days
683 were rarely observed at the 12 background sites in this study. The moderately polluted and polluted
684 days were still mainly concentrated in the winter in the megacities of the GZP and NCP and also
685 occurred in the winter in the megacities of the YRD and SWCR. In addition, March to June and
686 September to October were periods with high occurrences of polluted days. Dust storms from
687 northern China (March to April), biomass burning after crop harvests (May to June and September
688 to October) and worsening dispersion conditions after the summers likely accounted for the
689 polluted days (Cheng et al., 2014; Fu et al., 2014). The majority of slightly polluted days occurred
690 from June to September, except at several urban sites in southern China. The mass level of 35-75
691 $\mu g/m^3$ was considered a low level of pollution for the entire year, illustrating that the summer and
692 early autumn experienced cleaner conditions.

693   The mean percentile compositions of the major components in $PM_{2.5}$ at different pollution
694 levels from four paired urban-background sites are shown in Fig. 8. With the pollution level
695 increased from clean to moderately polluted, the EC fraction in Beijing decreased slightly, the OM
696 fraction decreased significantly, and the sulfate and nitrate contributions increased sharply (Fig.
697 8a). The same chemical evolution of the $PM_{2.5}$ was also observed at the background site of
698 Xinglong, suggesting that regional transport plays a vital role in the formation of the slightly and
699 moderately polluted days in the NCP. When the pollution level increased to heavily polluted,
700 however, the OM fraction further increased and was accompanied by increases of the sulfate and
701 nitrate contributions as well as decreases of the mineral dust contribution. This result indicates the
702 enhanced secondary transformation of gaseous pollutants (etc. SO_2, NOx, VOCs) during heavily
703 polluted periods, which is consistent with the findings of our previous study (Liu et al., 2016a),
704 which stated that regionally transported aerosols contribute the most during slightly and
705 moderately polluted days, while local origin secondary aerosols dominate the increases of fine
706 particles during heavily polluted days in Beijing. Unlike in Beijing, the contributions of OM and
707 EC were almost constant across the different pollution levels in Guangzhou, while the contribution
708 of the secondary inorganic aerosols (SIA) increased slightly (Fig. 8b). Interestingly, the nitrate
709 contribution increased faster than that of the sulfate when the pollution level increased from clean
710 to heavily polluted, similar to the patterns of Beijing, which may suggest the enhanced
711 contribution of local traffic emissions in these two cities during heavily polluted days. The
712 chemical evolution of $PM_{2.5}$ at the background site of PRD was similar to that of the urban site at
713 Guangzhou, although a significant contribution of SIA was observed when the pollution level
714 increased from clean to moderately polluted (34% vs. 58%). Note that the contribution of sulfate

715 increased sharply, suggesting that regional transports dominated the particle pollution during
716 heavily polluted days. Compared with Beijing, a reversed chemical evolution of $PM_{2.5}$ for the
717 different pollution levels was observed in Shenyang, with the OM fraction increasing sharply from
718 22% to 37%, while the SIA decreased slightly from 39% to 31% (Fig. 8c). Note that a steady
719 increase of sulfate from slightly polluted days to heavily polluted days was observed. These results
720 suggest that enhanced local emissions dominate the temporal evolution of $PM_{2.5}$ on polluted days
721 in Shenyang. A similar chemical evolution of $PM_{2.5}$ was found at the background site of Changbai
722 Mountain, which showed a significantly increased OM fraction and slightly decrease of SIA when
723 the pollution level increased from clean to slighted polluted, indicating the enhanced contribution
724 from local emissions like coal combustion for heating during slightly polluted days. Further
725 support for this pattern is seen in the increase of the EC fraction (Fig. 8 g). Similar to that in
726 Guangzhou, the contribution of OM was almost constant for different pollution levels in
727 Chongqing. In addition, a much higher contribution of SIA was observed, especially during the
728 heavily polluted days, which suggests the importance of the formation of SIA in driving $PM_{2.5}$
729 pollution in Chongqing. The background site of Gongga Mountain shows decreased contributions
730 of OM, EC, SIA and mineral dust when the pollution level increased from clean to slightly
731 polluted days, similar to the pattern observed in Xinglong. Note that the unaccounted-for fraction
732 was largely increased on slightly polluted days (33% vs. 10%), possibly due to the increase of
733 aerosol-bound water related to the hygroscopic growth of aerosols at high RH values on slightly
734 polluted days (Bian et al., 2014). These results suggest the different formation mechanisms of the
735 heavy pollution in the most polluted city clusters, and unique mitigation measures should be
736 developed for the different regions of China.
737
738 **4. Conclusions**
739   We have established a national-level network ("Campaign on atmospheric Aerosol REsearch"
740 network of China (CARE-China)) that conducted continuous monitoring of $PM_{2.5}$ mass
741 concentrations at 40 ground observation station, including 20 urban sites, 12 background sites and
742 8 rural/suburban sites. The average aerosol chemical composition was inferred from the filter
743 samples from six paired urban and background sites, which represent the largest megacities and
744 regional background areas in the five most polluted regions and the TAR of China. This study
745 presents the first long-term dataset including three-year observations of online $PM_{2.5}$ mass
746 concentrations (2012-2014) and one year observations of $PM_{2.5}$ compositions (2012-2013) from
747 the CARE-China network. One of the major purposes of this study was to compare and contrast
748 urban and background aerosol concentrations from nearby regions. The major findings include the
749 following:
750   (1) The average $PM_{2.5}$ concentration from 20 urban sites is 73.2 μg/m^3 (16.8-126.9 μg/m^3),
751 which is three times greater than the average value of 12 background sites (11.2-46.5 μg/m^3). The
752 highest $PM_{2.5}$ concentrations were observed at the stations on the Guanzhong Plain (GZP) and the
753 NCP. The $PM_{2.5}$ pollution is also a serious problem for the industrial regions of northeastern China
754 and the Sichuan Basin and is a relatively less serious problem for the YRD and the PRD. The
755 background $PM_{2.5}$ concentrations of the NCP, YRD and PRD were comparable to those of the
756 nearby urban sites, especially for the PRD. A distinct seasonal variability of the $PM_{2.5}$ is observed,

757 presenting peaks during the winter and minima during the summer at the urban sites, while the
758 seasonal variations of $PM_{2.5}$ at the background sites vary in different part of China. Bimodal and
759 unimodal diurnal variation patterns were identified at both the urban and background stations.

760   (2) The major $PM_{2.5}$ constituents across all the urban sites are OM (26.0%), SO_4^{2-}(17.7%),
761 mineral dust (11.8%), NO_3^- (9.8%), NH_4^+ (6.6%), EC (6.0%), Cl^- (1.2%) at 45% RH and residual
762 matter (20.7%). Similar chemical compositions of $PM_{2.5}$ were observed for the background sites
763 and were associated with higher fractions of OM (33.2%) and lower fractions of NO_3^- (8.6%) and
764 EC (4.1%). Analysis of filter samples reveals that several $PM_{2.5}$ chemical components varied by
765 more than an order of magnitude between sites. For urban sites, the OM ranges from 12.6 $\mu g/m^3$
766 (Lhasa) to 23.3 $\mu g/m^3$ (Shenyang), the SO_4^{2-} ranges from 0.8 $\mu g/m^3$ (Lhasa) to 19.7 $\mu g/m^3$
767 (Chongqing), the NO_3^- ranges from 0.5 $\mu g/m^3$ (Lhasa) to 11.9 $\mu g/m^3$ (Shanghai) and the EC ranges
768 from 1.4 $\mu g/m^3$ (Lhasa) to 7.1 $\mu g/m^3$ (Guangzhou). The $PM_{2.5}$ chemical species of the background
769 sites exhibit larger spatial heterogeneities than those of the urban sites, suggesting the different
770 contributions from regional anthropogenic and natural emissions and from the long-range
771 transport to background areas.

772   (3) Notable seasonal variations of $PM_{2.5}$ polluted days were observed, especially for the
773 megacities in east-central China, resulting in frequent heavy pollution episodes occurring during
774 the winter. The evolution of the chemical compositions of the $PM_{2.5}$ on polluted days was similar
775 for the urban and nearby background sites, suggesting the significant regional pollution
776 characteristics of the most polluted areas of China. However, the chemical species dominating the
777 evolutions of heavily polluted events were different in these areas. While sharply increasing
778 contributions of SIA and decreasing or constant contributions of OM during heavily polluted days
779 were observed in Beijing, Guangzhou and Chongqing, the reverse contributions of secondary
780 inorganic aerosol and OM were observed during the heavily polluted days of Shenyang. These
781 results suggest that unique mitigation measures should be developed for different regions of
782 China.

783   The seasonal and spatial patterns of urban and background aerosols emphasize the
784 importance of understanding the variabilities of the concentrations of major aerosol species and
785 their contributions to the $PM_{2.5}$ budget. Comparisons of $PM_{2.5}$ chemical compositions from urban
786 and background sites of adjacent regions provided meaningful insights into aerosol sources and
787 transport and into the role of urban influences on nearby rural regions. The integration of data
788 from 40 sites from the CARE-China network provided an extensive spatial coverage of fine
789 particle concentrations near the surface and could be used to validate model results and implement
790 effective air pollution control strategies.

791

799   References

800   Bell, M.L., Dominici, F., Ebisu, K., Zeger, S.L., and Samet, J.M.: Spatial and temporal variation in $PM_{2.5}$ chemical

801   composition in the United States for health effects studies. Environ Health Perspect. 115, 989-995, 2007.

802   Bian, Y. X., Zhao, C. S., Ma, N., Chen, J., and Xu, W. Y.: A study of aerosol liquid water content based on

803   hygroscopicity measurements at high relative humidity in the North China Plain. Atmos. Chem. Phys., 14,

804   6417-6426, 2014.

805   Boyouk, N., Léon, J.-F., Delbarre, H., Podvin, T., and Deroo, C.: Impact of the mixing boundary layer on the

806   relationship between $PM_{2.5}$ and aerosol optical thickness, Atmos. Environ., 44(2), 271-277, 2010.

807   Chan, C. K., and Yao X.: Air pollution in mega cities in China, Atmos. Environ., 42(1), 1-42, 2008.

808   Chen, W. H., Wang, X. M., Zhou, S. Z., Cohen, J. B., Zhang, J., Wang, Y., Chang, M., Zeng, Y., Liu, Y., Ling, Z.,

809   Liang, G., Qiu, X.: Chemical Composition of $PM_{2.5}$ and its Impact on Visibility in Guangzhou, Southern China.

810   Aerosol Air Qual. Res., 16, 2349-2361, 2016.

811   Chen, Y., Xie, S. D., Luo, B., and Zhai, C. Z.: Particulate pollution in urban Chongqing of southwest China:

812   Historical trends of variation, chemical characteristics and source apportionment. Sci. Total Environ., 584-585,

813   523-534, 2017.

814   Chen, Z., Wang, J.-N., Ma, G.-X., and Zhang, Y.-S.: China tackles the health effects of air pollution, Lancet, 382,

815   1959-1960, 2013.

816   Cheng, Z.,Wang, S., Fu, X.,Watson, J.G., Jiang, J., et al., Impact of biomass burning on haze pollution in the

817   Yangtze River delta, China: a case study in summer 2011. Atmos. Chem. Phys. 14 (9), 4573-4585, 2014.

818   Cheng, Z., Luo, L., Wang, S., Wang, Y., Sharma, S., Shimadera, H., Wang, X., Bressi, M., Maura de Miranda, R.,

819   Jiang, J., Zhou, W., Fajardo, O., Yan, N., Hao, J.: Status and characteristics of ambient $PM_{2.5}$ pollution in global

820   megacities. Environ. Int., 89-90, 212-221, 2016.

821   Cong, Z., Kang, S., Luo, C., Li, Q., Huang, J., et al., Trace elements and lead isotopic composition of PM_{10} in

822   Lhasa, Tibet. Atmos. Environ. 45, 6210-6215, 2011.

823   Dickerson, R.R., Li, C., Li, Z., Marufu, L.T., Stehr, J.W., McClure, B., Krotkov, N., Chen, H., Wang, P., Xia, X.,

824   Ban, X., Gong, F., Yuan, J., and Yang, J.: Aircraft observations of dust and pollutants over northeast China: insight

825   into the meteorological mechanisms of transport. Journal of Geophysical Research 112, D24S90,.

826   http://dx.doi.org/10.1029/2007JD008999, 2007.

827   Eeftens, M., Tsai, M.-Y., Ampe, C., Anwander, B., Beelen, R., Bellander, T., Cesaroni, G., Cirach, M., Cyrys, J.,

828   Hoogh, K. D., Nazelle, A. D., Vocht, F. D., Declercq, C., Dedele, A., Eriksen, K., Galassi, C., Grazuleviciene, R.,

829   Grivas, G., Heinrich, J., Hoffmann, B., Iakovides, M., Ineichen, A., Katsouyanni, K., Korek, M., Krämer, U.,

830   Kuhlbusch, T., Lanki, T., Madsen, C., Meliefste, K., Mölter, A., Moslerm, G., Nieuwenhuijsen, M., Oldenwening,

831   M., Pennanen, A., Probst-Hensch, N., Quass, U., Raaschou-Nielsen, O., Ranzi, A., Stephanou, E., Sugiri, D.,

832   Udvardy, O., Vaskövi, É., Weinmayr, G., Brunekreef, B., and Hoek, G.: Spatial variation of $PM_{2.5}$, PM_{10}, $PM_{2.5}$

833   absorbance and PM coarse concentrations between and within 20 European study areas and the relationship with

834   NO_2 – Results of the ESCAPE project, Atmos. Environ., 62, 303-317, 2012.

835   Fu, X., Wang, S. X., Zhao, B., Xing, J., Cheng, Z., Liu, H., and Hao, J. M.: Emission inventory of primary

836   pollutants and chemical speciation in 2010 for the Yangtze River Delta region, China. Atmos. Environ., 70, 39-50,

837   2013.

838   Fu, X., Wang, S. X., Cheng, Z., Xing, J., Zhao, B., Wang, J. D., et al., Source, transport and impacts of a heavy

839   dust event in the Yangtze River Delta, China, in 2011. Atmos. Chem. Phys. 14 (3), 1239-1254, 2014.

840   Gehrig, R. and Buchmann, B.: Characterising seasonal variations and spatial distribution of ambient PM_{10} and

841    $PM_{2.5}$ concentrations based on long-term Swiss monitoring data, Atmos. Environ., 37, 2571-2580, 2003.

842   Guo, S., Hu, M., Zamora, M. L., et al. Elucidating severe urban haze formation in China. Proc. Nat. Acad. Sci.

843   U.S.A. 111, 17373-17378, 2014.

844   Hand, J. L., Schichtel, B. A., Pitchford, M., Malm, W. C., and Frank, N. H.: Seasonal composition of remote and

845   urban fine particulate matter in the United States, J. Geophys. Res., 117, D05209, doi:10.1029/2011JD017122,

846   2012.

847   He, K. B., Yang, F. M., Ma, Y. L., Zhang, Q., Yao, X. H., Chan, C. K., Cadle, S., Chan, T., and Mulawa, P.: The

848   characteristics of $PM_{2.5}$ in Beijing, China, Atmos. Environ., 35(29), 4959-4970, 2001.

849   Hoffer, A., Gelencsér, A., Guyon, P., Kiss, G., Schmid, O., Frank, G. P., Artaxo, P. and Andreae, M. O.: Optical

850   properties of humic-like substances (HULIS) in biomass-burning aerosols. Atmos. Chem. Phys., 6, 3563-3570,

851   2006.

852   Huang, R. J., Zhang, Y., Bozzetti, C., et al. High secondary aerosol contribution to particulate pollution during haze

853   events in China. Nature, 514, 218-222, 2014.

854   Huang, Y., Li, L., Li, J., et al. A case study of the highly time-resolved evolution of aerosol chemical and optical

855   properties in urban Shanghai, China. Atmos. Chem. Phys., 13(8), 3931-3944, 2013.

856   IPCC: Climate Change 2013: The Physical Science Basis: Summary for Policymakers, Cambridge, UK, 2013.

857   Janssen, N. A. H., Fischer, P., Marra, M., Ameling, C., and Cassee, F. R.: Short-term effects of $PM_{2.5}$, PM_{10} and

858    $PM_{2.5-10}$ on daily mortality in the Netherlands. Sci. Total. Environ., 463-464, 20-26, 2013.

859   Li, L., Chen, C. H., Fu, J. S., Huang, C., Streets, D. G., Huang, H. Y., Zhang, G. F., Wang, Y. J., Jang, C. J., Wang,

860   H. L., Chen, Y. R., and Fu. J. M.: Air quality and emissions in the Yangtze River Delta, China. Atmos. Chem. Phys.,

861   11, 1621-1639, 2011

862   Li, Y. C., Yu, J. Z., Ho, S. S. H., Yuan, Z. B., Lau, A. K. H., and Huang X. F.: Chemical characteristics of $PM_{2.5}$ and

863   organic aerosol source analysis during cold front episodes in Hong Kong, China, Atmos. Res., 118, 41-51, 2012.

864   Liu, Z. R., Hu, B., Wang, L. L., Wu, F. K., Gao, W. K., and Wang, Y. S.: Seasonal and diurnal variation in

865   particulate matter (PM_{10} and $PM_{2.5}$) at an urban site of Beijing: analyses from a 9-year study. Environ. Sci. Pollut.

866   Res., 22, 627-642, 2015.

867   Liu, L., Zhang, X., Wang, S., Zhang, W., and Lu, X.: Bulk sulfur (S) deposition in China. Atmos. Environ. 135,

868   41-49, 2016b.

869   Liu, Z. R., Wang, Y. S., Hu, B., Ji, D. S., Zhang, J. K., Wu, F. K., Wan, X. and Wang, Y. H. Source appointment of

870   fine particle number and volume concentration during severe haze pollution in Beijing in January 2013, Environ.

871   Sci. Pollut. Res., 23(7), 6845-6860, doi:10.1007/s11356-015-5868-6, 2016a.

872   Liu, Z. R., Wang, Y. S., Liu, Q., Liu, L. N., and Zhang, D. Q.: Pollution Characteristics and Source of the

873   Atmospheric Fine Particles and Secondary Inorganic Compounds at Mount Dinghu in Autumn Season (in Chinese).

874   Environ. Sci., 32, 3160-3166, 2011.

875   Lu, Z., Streets, D. G., Zhang, Q., Wang, S., Carmichael, G. R., Cheng, Y.F., et al., Sulfur dioxide emissions in

876   China and sulfur trends in East Asia since 2000. Atmos. Chem. Phys. 10, 6311-6331, 2010.

877   Malm, W. C., Schichtel, B. A., Pitchford, M. L., Ashbaugh, L. L., and Eldred, R. A.: Spatial and monthly trends in

878   speciated fine particle concentration in the United States, J. Geophys. Res., 109, D03306,

879   doi:10.1029/2003JD003739, 2004.

880   Mamtimin, B., and Meixner, F. X.: Air pollution and meteorological processes in the growing dryland city of

881   Urumqi (Xinjiang, China). Sci. Total Environ., 409(7), 1277-1290, 2011.

882   Mao, Y. H., Liao, H., and Chen, H. S.: Impacts of East Asian summer and winter monsoons on interannual

883   variations of mass concentrations and direct radiative forcing of black carbon over eastern China. Atmos. Chem.

884   Phys., 17, 4799-4816, 2017.

885   Mauderly, J. L., and Chow, J. C.: Heath effects of organic aerosols, Inhal. Toxicol., 20, 257-288, 2008.

886   Niu, Z. C., Zhang, F. W., Chen, J. S., Yin, L. Q., Wang, S., and Xu, L. L.: Carbonaceous species in $PM_{2.5}$ in the

887   coastal urban agglomeration in the Western Taiwan Strait Region, China. Atmos. Res. 122, 102-110, 2013.

888   Oanh, N. T. K., Upadhyay, N., Zhuang, Y.-H., Hao, Z.-P., Murthy, D. V. S., Lestari, P., Villarin, J. T., Chengchua,

889   K., Co, H. X., Dung, N. T., and Lindgren, E. S.: Particulate air pollution in six Asian cities: Spatial and temporal

890   distributions, and associated sources, Atmos. Environ., 40, 3367-3380, doi:10.1016/j.atmosenv.2006.01.050, 2006.

891   Pan, Y. P., Wang, Y. S., Sun, Y., Tian, S. L., and Cheng, M. T.: Size-resolved aerosol trace elements at a rural

892   mountainous site in Northern China: Importance of regional transport, Sci. Total Environ., 461, 761-771, 2013.

893   Patashnick, H., and Rupprecht, E.: Continuous PM_{10} measurements using the tapered element oscillating

894   microbalance. J. Air Waste Manage., 41, 1079-1083, doi:10.1080/10473289.1991.10466903, 1991.

895   Putaud, J.-P., Van Dingenen, R., Alastuey, A., Bauer, H., Birmili, W., Cyrys, J., Flentje, H., Fuzzi, S., Gehrig, R.,

896   Hansson, H. C., Harrison, R. M., Herrmann, H., Hitzenberger, R., Hüglin, C., Jones, A. M., Kasper-Giebl, A., Kiss,

897   G., Kousa, A., Kuhlbusch, T. A. J., Löschau, G., Maenhaut, W., Molnar, A., Moreno, T., Pekkanen, J., Perrino, C.,

898   Pitz, M., Puxbaum, H., Querol, X., Rodriguez, S., Salma, I., Schwarz, J., Smolik, J., Schneider, J., Spindler, G., ten

899   Brink, H., Tursic, J., Viana, M., Wiedensohler, A., and Raes, F.: A European aerosol phenomenology – 3: Physical

900   and chemical characteristics of particulate matter from 60 rural, urban, and kerbside sites across Europe, Atmos.

901   Environ., 44, 1308–1320, doi:10.1016/j.atmosenv.2009.12.011, 2010.

902   Quan, J. N., Tie, X. X., Zhang, Q., Liu, Q., Li, X., Gao, Y., and Zhao, D. L.: Characteristics of heavy aerosol

903   pollution during the 2012-2013 winter in Beijing, China, Atmos. Environ., 88, 83-89, 2014.

904   Seinfeld, J. H., and Pandis, S. N.: Atmospheric Chemistry and Physics: from Air Pollution to Climate Change.

905   Wiley, New York, USA, 2016.

906   Sun, Q. H., Hong, X. R., and Wold, L. E.: Cardiovascular Effects of Ambient Particulate Air Pollution Exposure,

907   Circulation, 121(25), 2755-2765, 2010.

908   Tao, J., Zhang, L. M., Ho, K. F., Zhang, R. J., Lin, Z. J., Zhang, Z. S., Lin, M., Cao, J. J., Liu, S. X., and Wang, G.

909   H.: Impact of $PM_{2.5}$ chemical compositions on aerosol light scattering in Guangzhou - the largest megacity in

910   South China, Atmos. Res., 135, 48-58, 2014.

911   Tao, J., Zhang, L. M., Cao, J. J., Zhong, L. J., Chen, D. S., Yang, Y. H., Chen, D. H., Chen, L. G., Zhang, Z. S., Wu,

912   Y. F., Xia, Y. J., Ye, S. Q., and Zhang, R. J.: Source apportionment of $PM_{2.5}$ at urban and suburban areas of the

913   Pearl River Delta region, south China - With emphasis on ship emissions. Sci. Total Environ., 574, 1559-1570,

914   2017.

915   Turpin, B. J., and Lim, H. J.: Species contributions to $PM_{2.5}$ mass concentrations: Revisiting common assumptions

916   for estimating organic mass, Aerosol Sci. Technol., 35, 602-610, doi:10.1080/02786820152051454, 2001.

917   Verma, R. L., Sahu, L. K., Kondo, Y., Takegawa, N., Han, S., Jung, J. S., Kim, Y. J., Fan, S., Sugimoto, N., Shammaa,

918   M. H., Zhang, Y. H. and Zhao, Y.: Temporal variations of black carbon in Guangzhou, China, in summer 2006.

919   Atmos. Chem. Phys., 10, 6471-6485, 2010.

920   Viana, M., X., Querol, A., Alastuey, F., Ballester, S., Llop, A., Esplugues, R., Fernandez-Patier, S., dos Santos, G.,

921   and Herce, M. D.: Characterising exposure to PM aerosols for an epidemiological study, Atmos. Environ., 42(7),

922   1552-1568, 2008.

923   Wan, X., Kang, S. C., Xin, J. Y., Liu, B., Wen, T. X., Wang, P. L., Wang, Y. S., and Cong, Z. Y.: Chemical

924   composition of size-segregated aerosols in Lhasa city, Tibetan Plateau. Atmos. Res., 174-175, 142-150, 2016.

925   Wang, Y. S., Yao, L., Wang, L. L., et al. Mechanism for the formation of the January 2013 heavy haze pollution
926   episode over central and eastern China. Sci. China: Earth Sci., 57, 14-25, doi: 10.1007/s11430-013-4773-4, 2014.

927   Wang, G. H., Zhou, B. H., Cheng, C. L., Cao, J. J., Li, J. J., Meng, J. J., Tao, J., Zhang, R. J., and Fu, P. Q.: Impact
928   of Gobi desert dust on aerosol chemistry of Xi'an, inland China during spring 2009: differences in composition and
929   size distribution between the urban ground surface and the mountain atmosphere, Atmos. Chem. Phys., 13(2),
930   819-835, 2013.

931   Wang, H. L., Qiao, L. P., Lou, S. R., Zhou, M., Ding, A.J., Huang, H. Y., Chen, J. M., Wang, Q., Tao, S. K., Chen,
932   C. H., Li, L., and Huang, C.: Chemical composition of $PM_{2.5}$ and meteorological impact among three years in
933   urban Shanghai, China, J. Clean. Prod., 112, 1302-1311, 2016.

934   Wang, Y. Q., Zhang, X. Y., Sun, J. Y., Zhang, X. C., Che, H. Z., and Li, Y.: Spatial and temporal variations of the
935   concentrations of PM_{10}, $PM_{2.5}$ and PM_1 in China. Atmos. Chem. Phys., 15, 13585-13598, 2015.

936   Wu, F. K., Yu, Y., Sun, J., Zhang, J. K., Wang, J., Tang, G. Q., and Wang, Y. S.: Characteristics, source
937   apportionment and reactivity of ambient volatile organic compounds at Dinghu Mountain in Guangdong Province,
938   China. Sci. Total Environ., 548-549, 347-359, 2016.

939   Xia, X. A., Chen, H. B., Wang, P. C., Zhang, W. X., Goloub, P., Chatenet, B., Eck, T. F., and Holben, B. N.:
940   Variation of column-integrated aerosol properties in a Chinese urban region, J. Geophys. Res.-Atmos., 111,
941   D05204, doi:10.1029/2005JD006203, 2006.

942   Xin, J., Wang, Y., Wang, L., Tang, G., Sun, Y., Pan, Y., and Ji, D.: Reductions of $PM_{2.5}$ in Beijing-Tianjin-Hebei
943   urban agglomerations during the 2008 Olympic Games, Adv. Atmos. Sci., 29(6), 1330-1342, 2012.

944   Xing, L., Fu, T. M., Cao, J. J., Lee, S. C., Wang, G. H., Ho, K. F., Cheng, M. C., You, C. F., Wang, T. J.: Seasonal
945   and spatial variability of the OM/OC mass ratios and high regional correlation between oxalic acid and zinc in
946   Chinese urban organic aerosols. Atmos. Chem. Phys., 13, 4307-4318, 2013.

947   Xu, J. S., Xu, M. X., Snape, C., He, J., Behera, S. N., Xu, H. H., Ji, D. S., Wang, C. J., Yu, H., Xiao, H., Jiang, Y. J.,
948   Qi, B., Du, R. G.: Temporal and spatial variation in major ion chemistry and source identification of secondary
949   inorganic aerosols in Northern Zhejiang Province, China. Chemosphere, 179, 316-330, 2017.

950   Yang, F., Tan, J., Zhao, Q., Du, Z., He, K., Ma, Y., Duan, F., and Chen, G.: Characteristics of PM2.5 speciation in
951   representative megacities and across China, Atmos. Chem. Phys., 11(11), 5207-5219, 2011.

952   Ye, B., Ji, X., Yang, H., Yao, X., Chan, C. K., Cadle, S. H., Chan, T., and Mulawa, P. A.: Concentration and
953   chemical composition of $PM_{2.5}$ in Shanghai for a 1-year period, Atmos. Environ., 37, 499-510, 2003.

954   Zhang, C., Zhou, R., and Yang, S.: Implementation of clean coal technology for energy-saving and emission
955   reduction in Chongqing. Environment and Ecology in the Three Gorges (in Chinese), 3, 52-56, 2010.

956   Zhang, J. K., Sun, Y., Wu, F. K., Sun, J., and Wang, Y. S.: The characteristics, seasonal variation and source
957   apportionment of VOCs at Gongga Mountain, China. 88, 297-305, 2014c.

958   Zhang, L. W., et al. Long-term exposure to high particulate matter pollution and cardiovascular mortality: A
959   12-year cohort study in four cities in northern China, Environ. Int., 62, 41-47, 2014a.

960   Zhang, N. N., Cao, J.J., Liu, S.X., Zhao, Z.Z., Xu, H.M., and Xiao, S.: Chemical composition and sources of $PM_{2.5}$
961   and TSP collected at Qinghai Lake during summertime. Atmos. Res., 138, 213-222, 2014b.

962   Zhang, X. Y., Wang, Y. Q., Niu, T., Zhang, X. C., Gong, S. L., Zhang, Y. M., et al., Atmospheric aerosol
963   compositions in China: spatial/temporal variability, chemical signature, regional haze distribution and comparisons
964   with global aerosols. Atmos. Chem. Phys. 12 (2), 779-799, 2012.

965   Zhang, Y. L. and Cao, F: Fine particulate matter (PM2.5) in China at a city level. Sci. Rep., 5: 14884. 2015.

966   Zhao, M. F., Huang, Z. S., Qiao, T., Zhang, Y. K., Xiu, G. L., and Yu, J. Z.: Chemical characterization, the transport

967   pathways and potential sources of PM$_{2.5}$ in Shanghai: seasonal variations. Atmos. Res., 158, 66-78, 2015.

968   Zhao, P. S., Dong, F., Yang, Y. D., He, D., Zhao, X. J., Zhang, W. Z., Yao, Q., and Liu, H. Y.: Characteristics of

969   carbonaceous aerosol in the region of Beijing, Tianjin, and Hebei, China, Atmos. Environ., 71, 389-398, 2013a.

970   Zhao, X. J., Zhao, P. S., Xu, J., Meng, W., Pu, W. W., Dong, F., He, D., and Shi, Q. F.: Analysis of a winter regional

971   haze event and its formation mechanism in the North China Plain, Atmos. Chem. Phys., 13(11), 5685-5696, 2013b.

972   Zheng, J., Zhang, L., Che, W., Zheng, Z., and Yin, S.: A highly resolved temporal and spatial air pollutant emission

973   inventory for the Pearl River Delta region, China and its uncertainty assessment. Atmos. Environ. 43, 5112-5122,

974   2009.

975   Zhou, S. Z., et al. Formation of secondary organic carbon and long-range transport of carbonaceous aerosols at

976   Mount Heng in South China, Atmos. Environ., 63, 203-212, 2012.

977   Zimmermann, R.: Aerosols and health: a challenge for chemical and biological analysis. Anal Bioanal Chem., 407,

978   5863-5867, 2015.

979   Zou, X. K., and Zhai, P. M.: Relationship between vegetation coverage and spring dust storms over northern China.

980   J. Geophys. Res.109, D03104, doi:10.1029/2003JD003913, 2004.

981

Table 1 Geographic information and three-year mean $PM_{2.5}$ concentration of the monitor stations.

Station/Code	Latitude, Longitude	Altitude(m)	Station type	Mean(μg/m3)	N(day)
Beijing/BJC	39.97 °N, 116.37 °E	45	Northern city	69.4±54.8	1077
Cele/CLD	37.00 °N, 80.72 °E	1306	Northwestern country	126.9±155.4	600
Changbai Mountain/CBM	42.40 °N, 128.01 °E	738	Northeastern background	17.6±12.6	807
Changsha/CSC	28.21 °N, 113.06 °E	45	Central city	77.9±45.4	1045
Chengdu/CDC	30.67 °N, 104.06 °E	506	Southwestern city	102.2±66.2	1008
Chongqing/CQC	29.59 °N, 106.54 °E	259	Southwestern city	65.1±35.8	972
Dinghu Mountain/DHM	23.17 °N, 112.50 °E	90	Pearl River Delta background	40.1±25.0	954
Dunhuang/DHD	40.13 °N, 94.71 °E	1139	Desert town	86.2±94.3	726
Fukang/FKZ	44.28 °N, 87.92 °E	460	Northwestern country	69.9±69.6	960
Gongga Mountain/GGM	29.51 °N, 101.98 °E	1640	Southwestern background	25.5±15.5	869
Guangzhou/GZC	23.16 °N, 113.23 °E	43	Southern city	44.1±23.8	772
Hailun/HLA	47.43 °N, 126.63 °E	236	Northeastern country	41.6±45.0	1076
Hefei/HFC	31.86 °N, 117.27 °E	24	Eastern city	80.4±45.3	909
Ji'nan/JNC*	36.65 °N, 117.00 °E	70	Northern city	107.8±57.4	701
Kunming/KMC	25.04 °N, 102.73 °E	1895	Southwestern city	47.0±25.2	967
Lhasa/LSZ	29.67 °N, 91.33 °E	3700	Tibet city	30.6±21.3	600
Lin'an/LAZ*	30.30 °N, 119.73 °E	139	Eastern background	46.5±27.2	1086
Mount Everest/ZFM	28.21 °N, 86.56 °E	4700	Tibet background	24.4±25.1	390
Namtso/NMT	30.77 °N, 90.98 °E	4700	Tibet background	11.2±6.9	499
Nagri/ALZ	32.52 °N, 79.89 °E	4300	Tibet background	19.5±12.4	72
Qianyanzhou/QYZ	26.75 °N, 115.07 °E	76	Southeastern country	52.1±28.4	927
Qinghai Lake/QHL	37.62 °N, 101.32 °E	3280	Tibet background	16.2±17.0	590
Sanya/SYB	18.22 °N, 109.47 °E	8	Southern island city	16.8±13.1	595
Shanghai/SHC	31.22 °N, 121.48 °E	9	Eastern city	56.2±59.4	822
Shapotou/SPD	37.45 °N, 104.95 °E	1350	Desert background	51.1±33.3	1016
Shenyang/SYC	41.50 °N, 123.40 °E	49	Northeastern city	77.6±41.2	926
Shijiazhuang/SJZ*	38.03 °N, 114.53 °E	70	Northern city	105.1±92.7	1031
Taipei/TBC	25.03 °N, 121.90 °E	150	Island city	22.1±10.7	1083
Taiyuan/TYC	37.87 °N, 112.53 °E	784	Northern city	111.5±74.9	987
Tianjin/TJC*	39.08 °N, 117.21 °E	9	Northern city	69.9±49.6	1034
Tongyu/TYZ	44.42 °N, 122.87 °E	160	Inner Mongolia background	24.5±24.5	757
Urumchi/URC	43.77 °N, 87.68 °E	918	Northwestern city	104.1±145.2	776
Wuxi/WXC	31.50 °N, 120.35 °E	5	Eastern city	65.2±36.8	1003
Xi'An/XAC	34.27 °N, 108.95 °E	397	Central city	125.8±108.2	1077
Xianghe/XHZ	39.76 °N, 116.95 °E	25	North China suburbs	83.7±62.3	1084
Xinglong/XLZ	40.40 °N, 117.58 °E	900	North China background	39.8±34.0	1035
Xishuangbanna/BNF	21.90 °N, 101.27 °E	560	Southwestern rain forest	25.0±18.7	707
Yantai/YTZ	36.05 °N, 120.27 °E	47	East China sea coast city	51.1±36.7	915
Yucheng/YCA	36.95 °N, 116.60 °E	22	North China country	102.8±61.8	1008
Zangdongnan/ZDN	29.77 °N, 94.73 °E	2800	Southern Tibet forest	12.3±8.0	475

983   Table 2 Summary of the concentrations of $PM_{2.5}$ and its components ($\mu g/m^3$) in urban and
984   background sites.

Station	$PM_{2.5}$	OM	EC	NO_3^-	SO_4^{2-}	NH_4^+	MD*	Cl^-	Unaccounted
Urban sites									
Beijing(n=88)	71.7	19.1	4.1	9.3	11.9	5.3	4.7	0.7	16.5
Shanghai(n=120)	68.4	17.1	2.0	11.9	13.6	5.8			18.1
Guangzhou(n=106)	75.3	16.7	7.1	7.2	13.1	4.8	7.3	1.0	18.1
Lhasa(n=60)	36.4	12.6	1.4	0.5	0.8	0.4	11.6	0.3	8.8
Shenyang(n=36)	81.8	23.3	5.2	4.6	13.2	4.5	9.2	1.4	20.4
Chongqing(n=56)	73.5	17.2	4.8	6.5	19.7	6.1	7.4	0.6	11.2
Background sites									
Xinglong(n=42)	42.6	12.4	1.5	3.7	8.4	3.4	5.0	0.3	7.9
Lin'an(n=60)	66.3	21.7	2.9	8.7	11.2	7.3	2.0	0.6	11.9
Dinghu Mountain(n=36)	40.1	11.6	2.0	4.5	10.1	4.0	3.8	0.5	3.6
Namsto(n=35)	9.5	3.4	0.2	0.1	0.4	0.4	3.9	0.1	1.1
Changbai Mountain(n=52)	23.3	8.9	0.9	1.1	3.3	1.8	3.7	0.2	3.5
Gongga Mountain(n=36)	32.2	13.1	1.1	0.4	4.7	1.7	3.2	0.4	7.7

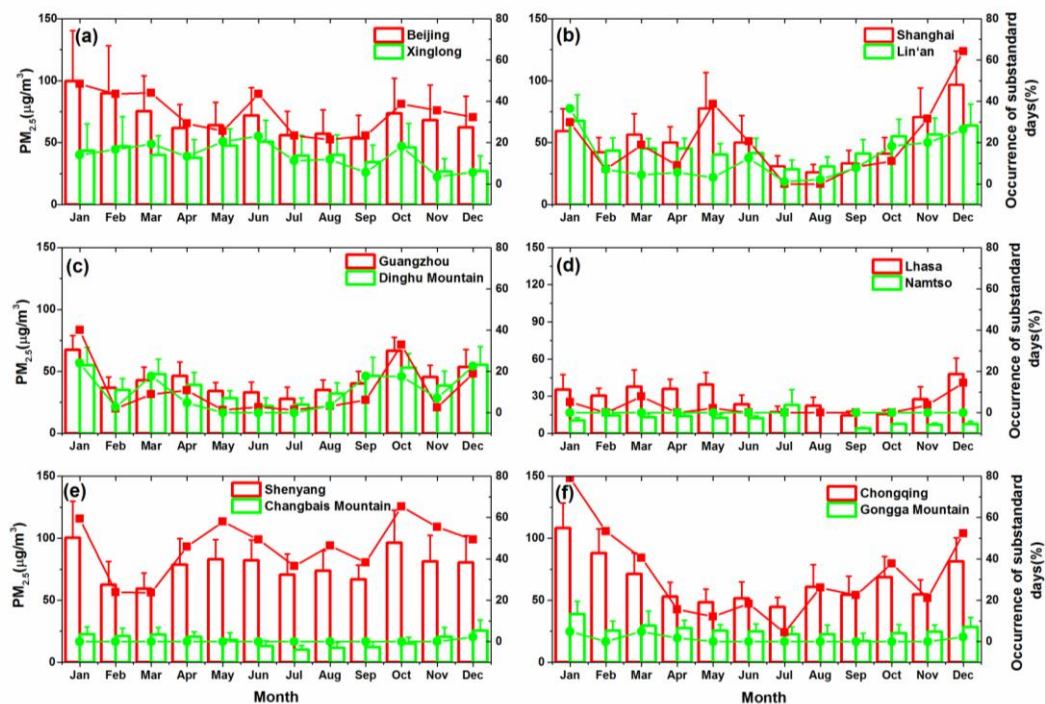985   *MD: mineral dust

986
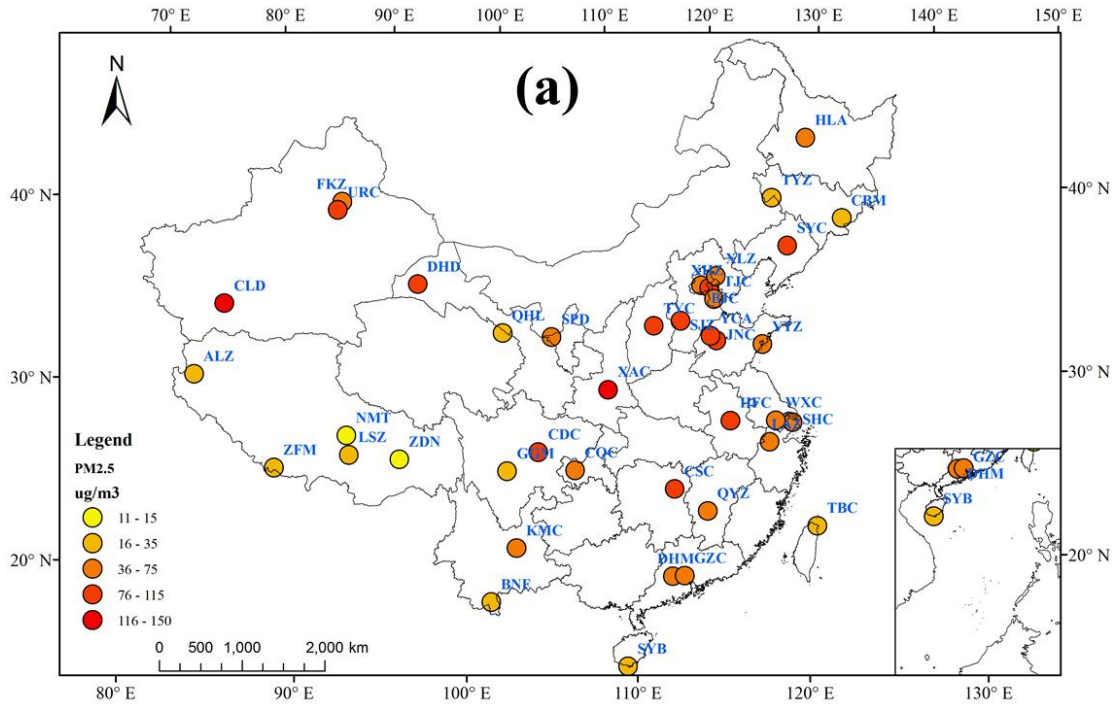
987
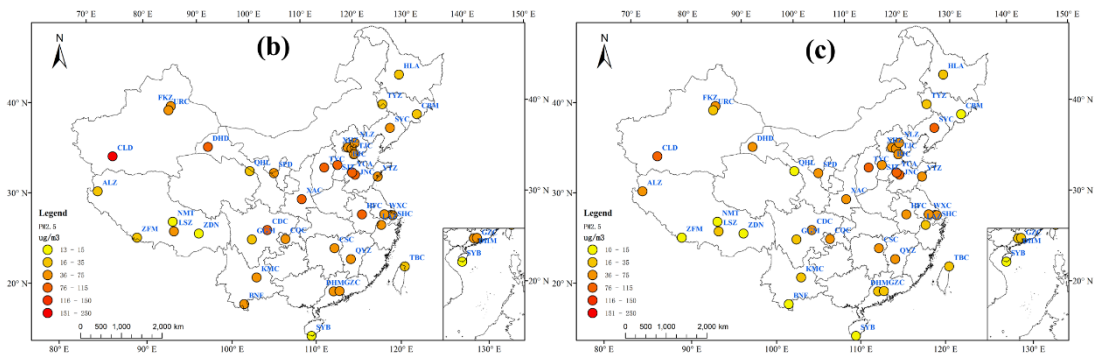
988
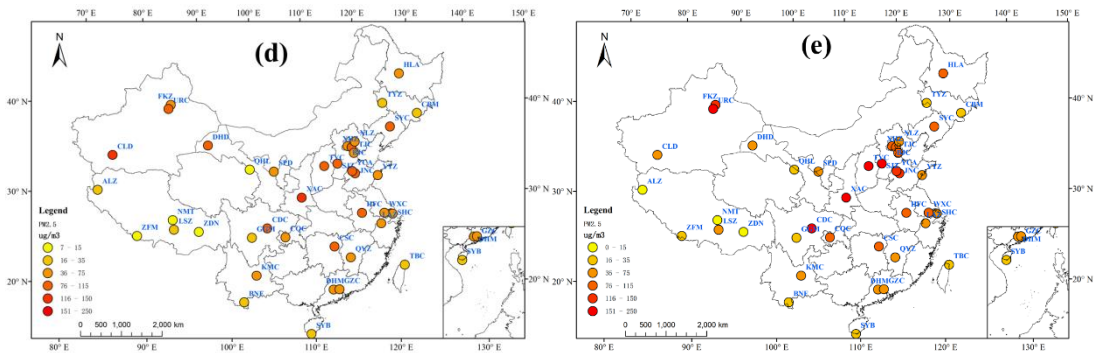
989

990 Fig.1. Locations and the averaged PM$_{2.5}$ concentrations of the forty monitor stations during (a) the
991 year of 2012-2014, (b) spring, (c) summer, (d) autumn and (e) winter

992

993

994

995
996 Fig.2. Monthly average PM$_{2.5}$ concentration (histogram, left coordinate) and the occurrence of
997 substandard days in each month (dotted line, right coordinate) at urban and background sites in
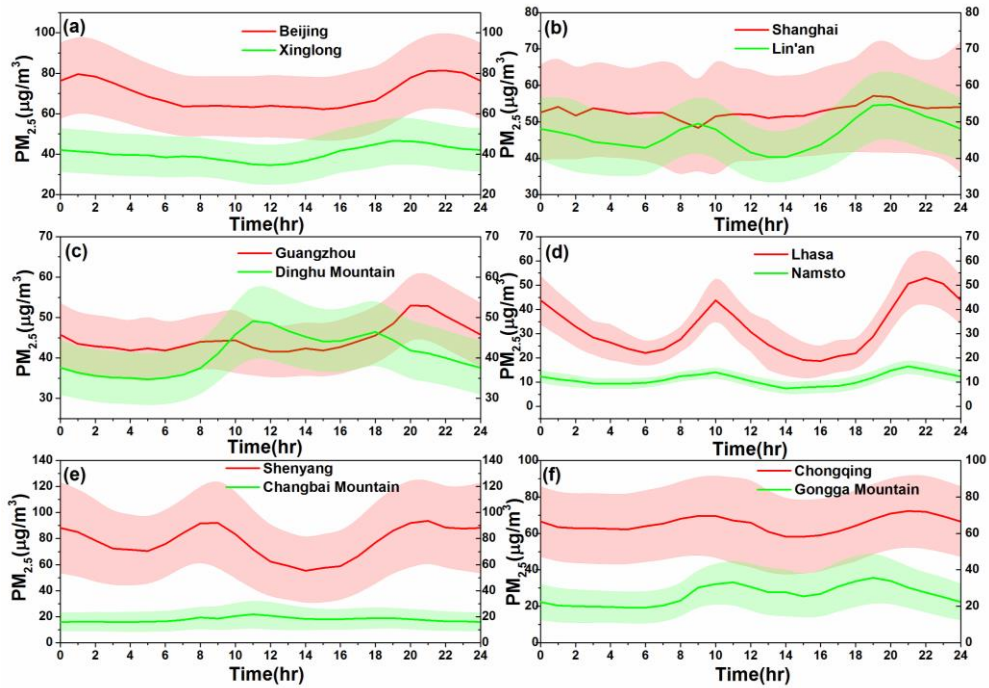998 (a)North China plain, (b)Yangtze River delta, (c) Pearl River delta, (d)Tibetan Autonomous Region ,
999 (e) Northeast China Region and (f) Southwestern China Region. The error bar stands for the
1000 standard deviation.
1001

1002

1003   Fig.3 Diurnal cycles of PM$_{2.5}$ at six paired urban and background sites in (a)North China plain,

1004   (b)Yangtze River delta, (c) Pearl River delta, (d)Tibetan Autonomous Region, (e) Northeast China

1005   Region and (f) Southwestern China Region.

1006
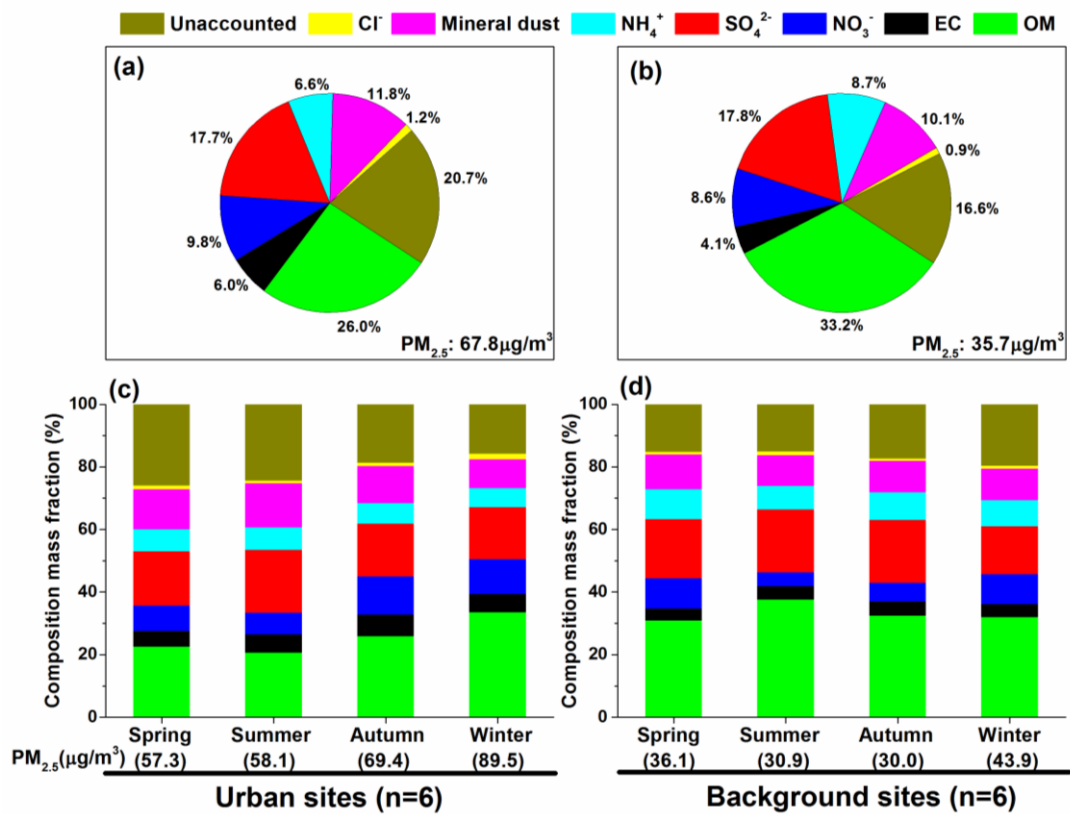
1007
1008 Fig.4 Average chemical composition and its seasonal variations of $PM_{2.5}$ in (a, c) urban sites and (b,
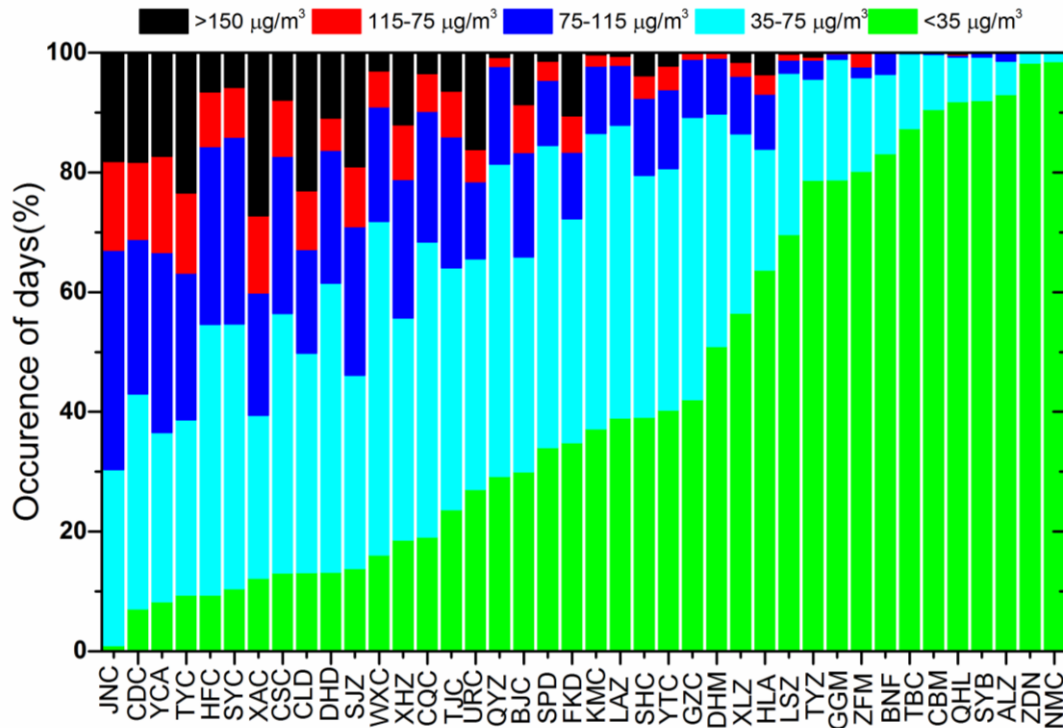1009 d) background sites.
1010
1011

1012
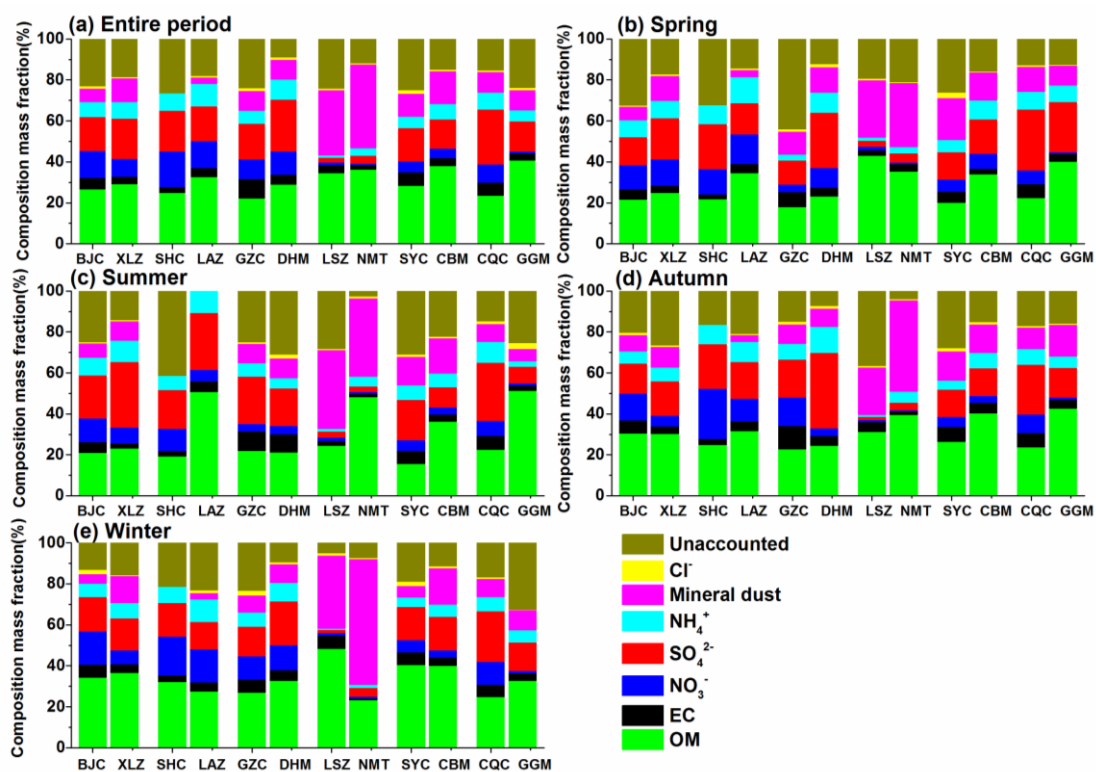
1013
1014   Fig.5 Average chemical composition of PM$_{2.5}$ in (a) urban sites and (b) background sites.

1015

1016

1017   Fig.6 Days separated by the threshold values of the "Ambient Air Quality Standard" (AAQS)

1018   (GB3095-2012) of China guideline. The threshold values of 35, 75, 115 and 150μg/m^3 used for the

1019   daily concentration ranges are represented as clean (<35μg/m^3), slightly polluted (35-75μg/m^3),

1020   moderated polluted (75-115μg/m^3), polluted (115-150μg/m^3) and heavily polluted (>150μg/m^3),

1021   which suggested by the guideline of the AAQS.

1022
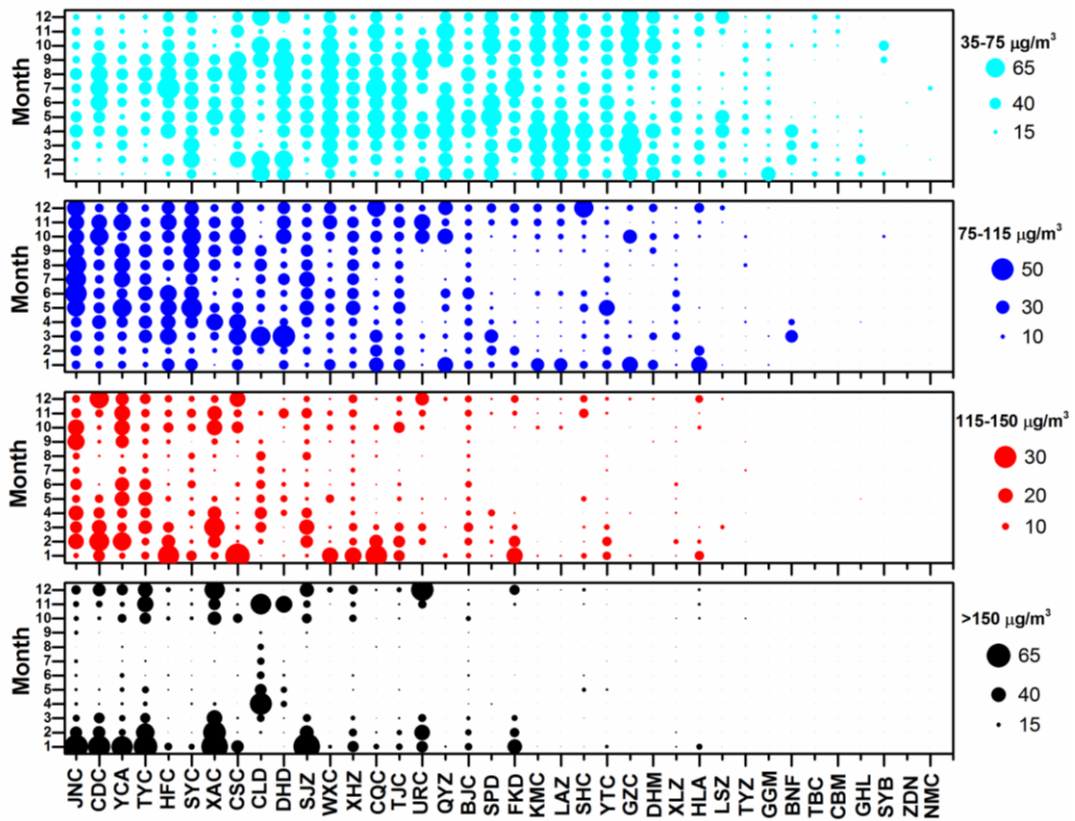
1023
1024 Fig.7 Monthly distribution of the occurrence of the polluted days exceeding the "Ambient Air
1025 Quality Standard" (AAQS) (GB3095-2012) of China. The symbol size represents the occurrences
1026 of polluted days for the corresponding month. The symbol color represents the different mass range.
1027 The sites of Nagri and Mount Everest are excluded because of the small sample size.
1028
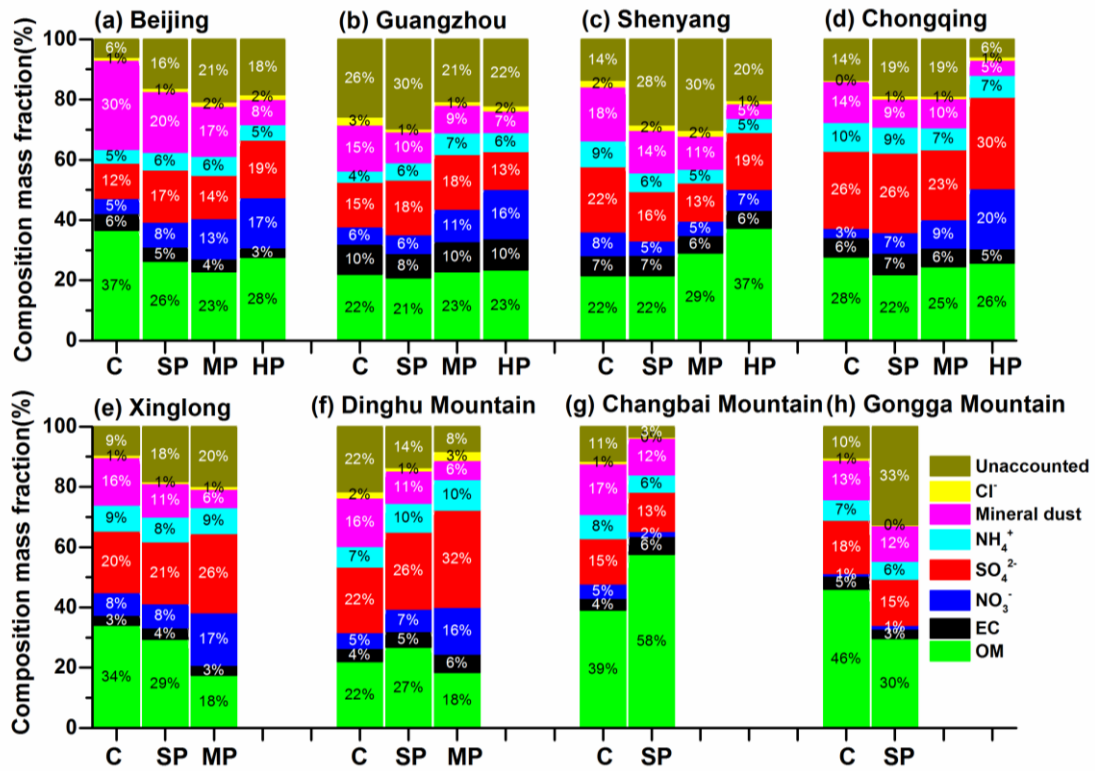
1029
1030 Fig. 8 Average chemical composition of $PM_{2.5}$ with respect to pollution level. The C, SP, MP and HP
1031 is related to clean (daily $PM_{2.5}$ <35 μg/m^3), slightly polluted (35 μg/m^3<daily $PM_{2.5}$ <75 μg/m^3),
1032 moderated polluted (75 μg/m^3<daily $PM_{2.5}$ <150 μg/m^3) and heavily polluted (daily $PM_{2.5}$ >150
1033 μg/m^3).
1034
1035